Acknowledgments This work was partly supported by the Histiocytosis Association of America (HAA grant 2009); a Grant-in-aid for Scientific Research (C) 23590426 from the Japanese Ministry of Education, Science, Sports and Culture; Grant for Research on Measures for Intractable Diseases from the Ministry of Health, Labor and Welfare of Japan; and a 2011 research grant from the Japan LCH Study Group. We thank Dr. Katsumi Higaki and Dr. Katsumi Nagata (Research Center for Bioscience and Technology, Tottori University) for their help with confocal microscopy and LC/MRM-MS.

Conflict of interest The authors declare that they have no conflict of interest.

References

1. Stawell, R (1921) Fabre's book of insects—retold from Alexander Teixeira de Mattos' translation of Fabre's "Souvenirs entomologiques". Dodd, Mead and Company, Inc. http://www.naderlibrary.com/lit.fabreinsectstoc.htm. Accessed 21 Sep 2012
2. Weitzman S, Egeler RM (2005) Histiocytic disorders of children and adults. Cambridge University Press, Cambridge
3. Jaffe R, Weiss LM, Fachetti (2008) Tumours derived from Langerhans cells. In: Swerdlow SH, Campo E, Harris NL, Jaffe ES, Pileri SA, Stein H, Thiele J, Vardiman JW (eds) WHO classification of tumours of haematopoietic and lymphoid tissues, 4th edn. WHO classification of tumours, Volume 2. International Agency for Research on Cancer, Lyon, pp 358–360
4. Willman CL, Busquet L, Griffith BB, Favara BE, McClain KL, Duncan MH, Gilliland DG (1994) Langerhans'-cell histiocytosis (histiocytosis X): a clonal proliferative disease. N Engl J Med 331:154–160
5. Yu RC, Chu C, Buluwela L, Chu AC (1994) Clonal proliferation of Langerhans cells in Langerhans cell histiocytosis. Lancet 343:767–768
6. Murakami I, Gogusev J, Fournet JC, Glorion C, Jaubert F (2002) Detection of molecular cytogenetic aberrations in Langerhans cell histiocytosis of bone. Hum Pathol 33:555–560
7. Badalian-Very G, Vergilio JA, Degar BA, MacConaill LE, Brandner B, Calicchio ML, Kuo FC, Ligon AH, Stevenson KE, Kehoe SM, Garraway LA, Hahn WC, Meyerson M, Fleming MD, Rollins BJ (2010) Recurrent BRAF mutations in Langerhans cell histiocytosis. Blood 116:1919–1923
8. Yamaguchi S, Oki S, Kurisu K (2004) Surg Neurol 62:136–140, discussion 140-141
9. McElligott J, McMichael A, Sangüeza OP, Anthony E, Rose D, McLean TW (2008) Spontaneous regression of Langerhans cell histiocytosis in a neonate with multiple bony lesions. J Pediatr Hematol Oncol 30:85–86
10. Nagasaki K, Tsumanuma I, Yoneoka Y, Ogawa Y, Kikuchi T, Uchiyama M (2009) Spontaneous regression of isolated neurohypophyseal Langerhans cell histiocytosis with diabetes insipidus. Endocr J 56:721–725
11. Arenzana-Seisdedos F, Barbey S, Virelizier JL, Kornprobst M, Nezelof C (1986) Histiocytosis X. Purified (T6+) cells from bone granuloma produce interleukin 1 and prostaglandin E2 in culture. J Clin Invest 77:326–329
12. Barbey S, Gane P, Le Pelletier O, Nezelof C (1987) Histiocytosis X Langerhans cells react with antiinterleukin-2 receptor monoclonal antibody. Pediatr Pathol 7:569–574
13. de Graaf JH, Tamminga RY, Dam-Meiring A, Kamps WA, Timens W (1996) The presence of cytokines in Langerhans' cell histiocytosis. J Pathol 180:400–406
14. Emile JF, Peuchmaur M, Fraitag S, Bodemer C, Brousse N (1993) Immunohistochemical detection of granulocyte/macrophage colony-stimulating factor in Langerhans' cell histiocytosis. Histopathology 23:327–332
15. Emile JF, Tartour E, Brugières L, Donadieu J, Le Deist F, Charnoz I, Fischer A, Fridman WH, Brousse N (1994) Detection of GM-CSF in the sera of children with Langerhans' cell histiocytosis. Pediatr Allergy Immunol 5:162–163
16. Emile JF, Fraitag S, Andry P, Leborgne M, Lellouch-Tubiana A, Brousse N (1995) Expression of GM-CSF receptor by Langerhans' cell histiocytosis cells. Virchows Arch 427:125–129
17. Egeler RM, Favara BE, van Meurs M, Laman JD, Claassen E (1999) Differential In situ cytokine profiles of Langerhans-like cells and T cells in Langerhans cell histiocytosis: abundant expression of cytokines relevant to disease and treatment. Blood 94:4195–4201
18. Neumann C, Schaumburg-Lever G, Döpfer R, Kolde G (1988) Interferon gamma is a marker for histiocytosis X cells in the skin. J Invest Dermatol 91:280–282
19. Hogarty MD (2011) IL-17A in LCH: systemic biomarker, local factor, or none of the above? Mol Ther 19(8):1405–1406. doi:10.1038/mt.2011.150
20. Yousem SA, Colby TV, Chen YY, Chen WG, Weiss LM (2001) Pulmonary Langerhans' cell histiocytosis: molecular analysis of clonality. Am J Surg Pathol 25:630–636
21. Vassallo R, Walters PR, Lamont J, Kottom TJ, Yi ES, Limper AH (2010) Cigarette smoke promotes dendritic cell accumulation in COPD; a Lung Tissue Research Consortium study. Respir Res 11:45
22. Coury F, Annels N, Rivollier A, Olsson S, Santoro A, Speziani C, Azocar O, Flacher M, Djebali S, Tebib J, Brytting M, Egeler RM, Rabourdin-Combe C, Henter JI, Arico M, Delprat C (2008) Langerhans cell histiocytosis reveals a new IL-17A-dependent pathway of dendritic cell fusion. Nat Med 14:81–87
23. Allen CE, McClain KL (2009) Interleukin-17A is not expressed by CD207(+) cells in Langerhans cell histiocytosis lesions. Nat Med 15:483–484, author reply:484-485
24. Allen CE, Li L, Peters TL, Leung HC, Yu A, Man TK, Gurusiddappa S, Phillips MT, Hicks MJ, Gaikwad A, Merad M, McClain KL (2010) Cell-specific gene expression in Langerhans cell histiocytosis lesions reveals a distinct profile compared with epidermal Langerhans cells. J Immunol 184:4557–4567
25. Peters TL, McClain KL, Allen CE (2011) Neither IL-17A mRNA nor IL-17A protein are detectable in Langerhans cell histiocytosis lesions. Mol Ther 19(8):1433–1439. doi:10.1038/mt.2011.106
26. Makras P, Polyzos SA, Anastasilakis AD, Terpos E, Papatheodorou A, Kaltsas GA (2012) Is serum IL-17A a useful systemic biomarker in patients with Langerhans cell histiocytosis? Mol Ther 20(1):6–7. doi:10.1038/mt.2011.239
27. Gaffen SL (2009) Structure and signalling in the IL-17 receptor family. Nat Rev Immunol 9:556-567 Erratum (2009). Nat Rev Immunol 9:747
28. Hamada H, Garcia-Hernandez Mde L, Reome JB, Misra SK, Strutt TM, McKinstry KK, Cooper AM, Swain SL, Dutton RW (2009) Tc17, a unique subset of CD8 T cells that can protect against lethal influenza challenge. J Immunol 182:3469–3481
29. Iwakura Y, Ishigame H, Saijo S, Nakae S (2011) Functional specialization of interleukin-17 family members. Immunity 34:149–162
30. DeFranco A, Locksley R, Robertson M (2007) Immunity: the immune response in infectious and inflammatory disease. Oxford University Press, Oxford
31. Conti HR, Shen F, Nayyar N, Stocum E, Sun JN, Lindemann MJ, Ho AW, Hai JH, Yu JJ, Jung JW, Filler SG, Masso-Welch P, Edgerton M, Gaffen SL (2009) Th17 cells and IL-17 receptor signaling are essential for mucosal host defense against oral candidiasis. J Exp Med 206:299–311
32. Kawamura T, Nomura M, Tojo H, Fujii K, Hamasaki H, Mikami S, Bando Y, Kato H, Nishimura T (2010) Proteomic analysis of laser-

microdissected paraffin-embedded tissues: (1) stage-related protein candidates upon non-metastatic lung adenocarcinoma. J Proteomics 73:1089–1099
33. Colombo PC, Ashton AW, Celaj S, Talreja A, Banchs JE, Dubois NB, Marinaccio M, Malla S, Lachmann J, Ware JA, Le Jemtel TH (2002) Biopsy coupled to quantitative immunofluorescence: a new method to study the human vascular endothelium. J Appl Physiol 92:1331–1338
34. Murakami I, Oka T, Kuwamoto S, Kato M, Hayashi K, Gogusev J, Imamura T, Morimoto A, Imashuku S, Yoshino T (2011) Tyrosine phosphatase SHP-1 is expressed higher in multisystem than in single-system Langerhans cell histiocytosis by immunohistochemistry. Virchows Arch 459:227–234
35. Aricò M, Girschikofsky M, Généreau T, Klersy C, McClain K, Grois N, Emile JF, Lukina E, De Juli E, Danesino C (2003) Langerhans cell histiocytosis in adults. Report from the International Registry of the Histiocyte Society. Eur J Cancer 39:2341–2348
36. Emile JF, Wechsler J, Brousse N, Boulland ML, Cologon R, Fraitag S, Voisin MC, Gaulard P, Boumsell L, Zafrani ES (1995) Langerhans' cell histiocytosis. Definitive diagnosis with the use of monoclonal antibody O10 on routinely paraffin-embedded samples. Am J Surg Pathol 19:636–641
37. Hoek A, Allaerts W, Leenen PJ, Schoemaker J, Drexhage HA (1997) Dendritic cells and macrophages in the pituitary and the gonads. Evidence for their role in the fine regulation of the reproductive endocrine response. Eur J Endocrinol 136:8–24
38. Simons PJ, Delemarre FG, Drexhage HA (1998) Antigen-presenting dendritic cells as regulators of the growth of thyrocytes: a role of interleukin-1beta and interleukin-6. Endocrinology 139:3148–3156
39. Aliahmadi E, Gramlich R, Grützkau A, Hitzler M, Krüger M, Baumgrass R, Schreiner M, Wittig B, Wanner R, Peiser M (2009) TLR2-activated human langerhans cells promote Th17 polarization via IL-1beta, TGF-beta and IL-23. Eur J Immunol 39:1221–1230
40. Ryzhakov G, Lai CC, Blazek K, To KW, Hussell T, Udalova I (2011) IL-17 boosts proinflammatory outcome of antiviral response in human cells. J Immunol 187:5357–5362
41. Shimakage M, Sasagawa T, Kimura M, Shimakage T, Seto S, Kodama K, Sakamoto H (2004) Expression of Epstein-Barr virus in Langerhans' cell histiocytosis. Hum Pathol 35:862–868
42. Kawakubo Y, Kishimoto H, Sato Y, Yanagimoto K, Tsuruta T, Ogawa Y, Kameya T (1999) Human cytomegalovirus infection in foci of Langerhans cell histiocytosis. Virchows Arch 434:109-115 Erratum (1999). Virchows Arch 435:77
43. Leahy MA, Krejci SM, Friednash M, Stockert SS, Wilson H, Huff JC, Weston WL, Brice SL (1993) Human herpesvirus 6 is present in lesions of Langerhans cell histiocytosis. J Invest Dermatol 101:642–645
44. Glotzbecker MP, Dormans JP, Pawel BR, Wills BP, Joshi Y, Elkan M, Hodinka RL (2006) Langerhans cell histiocytosis and human herpes virus 6 (HHV-6), an analysis by real-time polymerase chain reaction. J Orthop Res 24:313–320
45. Jeziorski E, Senechal B, Molina TJ, Devez F, Leruez-Ville M et al (2008) Herpes-virus infection in patients with Langerhans cell histiocytosis: a case-controlled sero-epidemiological study, and in situ analysis. PLoS One 3(9):e3262. doi:10.1371/journal.pone.0003262
46. Foss HD, Herbst H, Araujo I, Hummel M, Berg E, Schmitt-Gräff A, Stein H (1996) Monokine expression in Langerhans' cell histiocytosis and sinus histiocytosis with massive lymphadenopathy (Rosai-Dorfman disease). J Pathol 179:60–65
47. Sylvester J, Liacini A, Li WQ, Zafarullah M (2004) Interleukin-17 signal transduction pathways implicated in inducing matrix metalloproteinase-3, -13 and aggrecanase-1 genes in articular chondrocytes. Cell Signal 16:469–476
48. Chen K, Pociask DA, McAleer JP, Chan YR, Alcorn JF, Kreindler JL, Keyser MR, Shapiro SD, Houghton AM, Kolls JK, Zheng M (2011) IL-17RA is required for CCL2 expression, macrophage recruitment, and emphysema in response to cigarette smoke. PLoS One 6:e20333
49. Raychaudhuri SP, Raychaudhuri SK, Genovese MC (2012) IL-17 receptor and its functional significance in psoriatic arthritis. Mol Cell Biochem 359:419–429
50. Lanone S, Zheng T, Zhu Z, Liu W, Lee CG, Ma B, Chen Q, Homer RJ, Wang J, Rabach LA, Rabach ME, Shipley JM, Shapiro SD, Senior RM, Elias JA (2002) Overlapping and enzyme-specific contributions of matrix metalloproteinases-9 and -12 in IL-13-induced inflammation and remodeling. J Clin Invest 110:463–474
51. Pouladi MA, Robbins CS, Swirski FK, Cundall M, McKenzie AN, Jordana M, Shapiro SD, Stämpfli MR (2004) Interleukin-13-dependent expression of matrix metalloproteinase-12 is required for the development of airway eosinophilia in mice. Am J Respir Cell Mol Biol 30(1):84–90
52. Hou P, Troen T, Ovejero MC, Kirkegaard T, Andersen TL, Byrjalsen I, Ferreras M, Sato T, Shapiro SD, Foged NT, Delaissé JM (2004) Matrix metalloproteinase-12 (MMP-12) in osteoclasts: new lesson on the involvement of MMPs in bone resorption. Bone 34:37–43
53. Mogulkoc N, Veral A, Bishop PW, Bayindir U, Pickering CA, Egan JJ (1999) Pulmonary Langerhans' cell histiocytosis: radiologic resolution following smoking cessation. Chest 115:1452–1455
54. Leonardi C, Matheson R, Zachariae C, Cameron G, Li L, Edson-Heredia E, Braun D, Banerjee S (2012) Anti-interleukin-17 monoclonal antibody ixekizumab in chronic plaque psoriasis. N Engl J Med 366:1190–1199
55. Papp KA, Leonardi C, Menter A, Ortonne JP, Krueger JG, Kricorian G, Aras G, Li J, Russell CB, Thompson EH, Baumgartner S (2012) Brodalumab, an anti-interleukin-17-receptor antibody for psoriasis. N Engl J Med 366:1181–1189
56. Morimoto A et al (2011) Comprehensive analyses of serum levels of cytokines/chemokines and growth factors in pediatric patients with Langerhans cell histiocytosis. Pediatr Blood Cancer 56:696

Human Pathology (2014) 45, 119–126

ELSEVIER

Human PATHOLOGY

www.elsevier.com/locate/humpath

Original contribution

Merkel cell polyomavirus DNA sequences in peripheral blood and tissues from patients with Langerhans cell histiocytosis☆,☆☆

Ichiro Murakami MD, PhD[a,*], Michiko Matsushita MT, MA[b], Takeshi Iwasaki MD[a], Satoshi Kuwamoto MD, PhD[a], Masako Kato MD, PhD[a], Yasushi Horie MD, PhD[c], Kazuhiko Hayashi MD, PhD[a], Toshihiko Imamura MD, PhD[d], Akira Morimoto MD, PhD[e], Shinsaku Imashuku MD, PhD[f], Jean Gogusev MD, PhD[g], Francis Jaubert MD, PhD[h], Katsuyoshi Takata MD, PhD[i], Takashi Oka PhD, DMSc[i], Tadashi Yoshino MD, PhD[i]

[a]*Division of Molecular Pathology, Faculty of Medicine, Tottori University, Yonago 683–8503, Japan*
[b]*Department of Pathobiological Science and Technology, School of Health Science, Faculty of Medicine, Tottori University, Yonago 683–8503, Japan*
[c]*Department of Pathology, Tottori University Hospital, Yonago 683–8503, Japan*
[d]*Department of Pediatrics, Kyoto Prefectural University of Medicine, Kyoto 602–8566, Japan*
[e]*Department of Pediatrics, Jichi Medical University School of Medicine, Shimotsuke 329–0498, Japan*
[f]*Division of Pediatrics and Hematology, Takasago-seibu Hospital, Takasago 676–0812, Japan*
[g]*Inserm U507 and U1016, Institut Cochin, 75014 Paris, France*
[h]*University of Paris Descartes (Paris V), 75006 Paris, France*
[i]*Department of Pathology, Okayama University Graduate School of Medicine, Dentistry and Pharmaceutical Sciences, Okayama 700–8530, Japan*

Received 23 April 2013; revised 29 May 2013; accepted 31 May 2013

Keywords:
Merkel cell polyomavirus;
Langerhans cell histiocytosis;
Langerhans cells;
Dermatopathic lymphadenopathy;
Multiplex quantitative real-time PCR

Summary Langerhans cell histiocytosis (LCH) is a group of granulomatous disorders in which abnormal Langerhans cells proliferate as either a localized lesion in a single bone or disseminated disease involving two or more organs or systems. Because the different LCH forms exhibit significantly elevated levels of inflammatory molecules, including pro-inflammatory cytokines and tissue-degrading enzymes, we investigated for a possible viral trigger in LCH pathogenesis. We looked for Merkel cell polyomavirus (MCPyV) in peripheral blood cells and tissues using quantitative real-time PCR and immunohistochemistry staining with anti-MCPyV large T-antigen antibody. Our findings revealed elevated amounts of MCPyV DNA in the peripheral blood cells of 2 of 3 patients affected by LCH with high-risk organ involvement (RO+) and absence of MCPyV DNA in the blood cells in all 12 LCH-RO− patients ($P = .029$). With lower viral loads (0.002-0.033 copies/cell), an elevated number of MCPyV DNA sequences was detected in 12 LCH tissues in comparison with control tissues obtained from

☆ Competing interests: The authors declare no competing financial interests.

☆☆ Funding/Support: This work was partly supported by a Grant-in-Aid for Scientific Research (C) 23590426 from the Japanese Ministry of Education, Science, Sports and Culture and by 2010 and 2011 research grants from the Japan LCH Study Group.

* Corresponding author.
E-mail address: ichiro.murakami.09@gmail.com (I. Murakami).

http://dx.doi.org/10.1016/j.humpath.2013.05.028

patients with reactive lymphoid hyperplasia (0/5; $P = .0007$), skin diseases not related to LCH in children younger than 2 years (0/11; $P = .0007$), or dermatopathic lymphadenopathy (5/20; $P = .0002$). The data, including frequent but lower viral loads and low large-T antigen expression rate (2/13 LCH tissues), suggest that development of LCH as a reactive rather than a neoplastic process may be related to MCPyV infection.

1. Introduction

Langerhans cell histiocytosis (LCH) is a neoplastic lesion characterized by uncontrolled clonal proliferation of Langerhans cells (LCs) in a tissue environment containing other lymphoid cells [1–3]. The disease differs widely in clinical presentation, from a localized lesion as a single-system (SS-LCH) disease to a severe disseminated multisystem form (MS-LCH) [4]. The latter form is frequent in children younger than 2 years, whereas SS-LCH is more common in children older than 2 years [5].

The liver, spleen, and bone marrow are considered high-risk organs for LCH, whereas skin, bone, lymph nodes, gastrointestinal tissue, pituitary gland, and central nervous system are considered low-risk organs [4]. Therefore, LCH is classified clinically as either affecting at least one high-risk organ (RO+) or involving only organs without high risk (LCH-RO−) [4]. Although most patients with LCH-RO+ develop MS-LCH, in some patients having only one high-risk organ involved, the clinical course is milder, with symptoms similar to those observed in SS-LCH [6,7].

Although numerous studies have attempted to classify the LCH subtypes anatomically, no clear-cut consensus has yet been reached. For example, mutations in the proto-oncogene *BRAF* were found in 57% of a series of 61 cases, but there was no significant relation between the mutations and the clinical course of the disease [3]. An interleukin (IL)-17A autocrine LCH model of the severity of the disease was proposed [8], yet conflicting data remain, creating what often is described as the IL-17A controversy [9,10]. More recently, our group proposed an IL-17A endocrine model, showing a specific pattern of expression of the IL-17A receptor (IL-17RA) in relation to LCH subtype [11]. In fact, the IL-17A/IL-17RA autocrine/endocrine loop appears important in host defense, in that IL-17A boosts the pro-inflammatory reaction against viral aggression [12,13]. In the same context, we previously reported higher expression of phosphatase SHP-1 (also known as Tyrosine-protein phosphatase non-receptor type 6) [14], which by itself might promote Toll-like receptor–activated production of antiviral molecules such as interferon type I in abnormal LCH cells [15].

The LCH subtypes are associated with the release of inflammatory molecules such as pro-inflammatory cytokines and tissue-degrading enzymes [8,11,14,16,17] that are produced by LCs in contact with pathogens [18]. The most characteristic lesions observed in patients with LCH are skin maculopapular excrescences that imply involvement of an unknown dermotropic virus [4]. One such agent inducing LCH proliferation might be the common dermotropic Merkel cell polyomavirus (MCPyV) [19–21], the major pathogenic agent of Merkel cell carcinoma (MCC) of the skin [22,23]. Histologically, LCs are located above the middle of the prickle cell layer of the epidermis, whereas the Merkel cells are mostly sited in the basal layer of the epidermis. It was previously proposed that LCs capture external pathogens by elongation of dendrites beyond the tight junction barrier and function as antigen-presenting cells [24]. External pathogens might be recognized primarily by LCs or by a precursor LC present in the skin and not by the Merkel cells, as presently alleged.

In this report, elevated numbers of MCPyV DNA sequences were detected in the blood in two of three patients clinically classified as LCH-RO+. Altogether, the findings could be an important additional argument supporting the view that LCs behave as candidate sanctuary cells for asymptomatic MCPyV despite active antibody synthesis and that this pathogenic agent is involved in the development of LCH.

2. Patients and methods

2.1. Patients, peripheral blood, and LCH tissue samples

This study was approved by the Institutional Review Board of Okayama University Graduate School of Medicine, Dentistry, and Pharmaceutical Sciences, Okayama, Japan, and the Faculty of Medicine, Tottori University, Yonago, Japan.

Peripheral blood samples were obtained from 15 patients affected by LCH (6 SS-LCH, 9 MS-LCH; 3 LCH-RO+, 12 LCH-RO−). A total of 13 tissue samples from patients with LCH (7 SS-LCH, 6 MS-LCH; 1 LCH-RO+, 12 LCH-RO−) also were analyzed. As controls, 5 tissue samples from patients with reactive lymphoid hyperplasia (RLH), 11 from patients with skin diseases not related to LCH, and 20 from patients with dermatopathic lymphadenopathy (DLA) characterized by localized paracortical proliferation of epidermal LCs in the lymph nodes were analyzed. All tissues were prepared as formalin-fixed, paraffin-embedded (FFPE) samples.

Some of the LCH blood and tissue samples were obtained from patients included in the Japan LCH Study Group Registry between 2002 and 2009. Other samples were harvested from

patients at Okayama University Hospital or Tottori University Hospital between 2002 and 2011. The histopathologic diagnosis was established by conventional staining of histologic sections supplemented by immunohistochemical profiling using anti-CD1a and anti-S100 antibodies [25]. Tissue samples were fixed in 10% neutral-buffered formalin and embedded in paraffin. For immunohistochemistry (IHC) analysis, the sections were deparaffinized in xylene and rehydrated in a graded ethanol series. Anti-CD1a antibody (monoclonal mouse antihuman [IgG1, κ], O10; DAKO Japan, Kyoto, Japan) was used at a 1:100 dilution and anti-S100 antibody (polyclonal rabbit, Z0311; DAKO Japan) was used at a 1:1000 dilution. Endogenous peroxidase activity was blocked by hydrogen peroxide. For CD1a immunostaining, antigen retrieval was performed by heating the slides in 0.01 M citrate-buffered solution, pH 6.0, in a pressure cooker at 98°C for 15 minutes. The slides were then incubated for 1 hour in 5% skim milk and for 3 hours at 37°C with the primary antibodies against CD1a or S100. Samples were then incubated with secondary antibodies for 1 hour at room temperature and stained using the DAKO EnVision+ system (DAKO Japan) and 3,3′-diaminobenzidine as a chromogen followed by hematoxylin as a counterstain. Lymph nodes or skin samples were used as controls throughout.

2.2. DNA extraction

DNA was extracted from peripheral blood mononuclear cells (PBMCs) of patients with LCH and from LCH, RLH, non-LCH dermal diseases and DLA tissues. Extraction of DNA from PBMCs was performed using the proteinase K and phenol/chloroform/isoamyl alcohol (25:24:1 v/v/v) procedure. For tissue samples, DNA was extracted from the different paraffin blocks using the QIAamp DNA FFPE Tissue Kit and Mini Kit following the manufacturer's protocols (QIAGEN GmbH, Hilden, Germany).

2.3. Laser capture microdissection and DNA extraction

Laser capture microdissection was performed using an LMD7000 microscope (Leica Microsystems GmbH, Wetzler, Germany). The LCH or DLA lesions (FFPE tissue) were previously stained by immunolabeling with anti-S100 antibodies. Stained uncovered slides were air dried. Using conventional staining and CD1a immunostaining as references, approximately 1000 positive and negative LCH cells were collected by microdissection into 200-μL low-binding plastic tubes. The DNA was extracted using a QIAamp DNA Micro Kit (QIAGEN GmbH).

2.4. Multiplex Q-PCR for MCPyV detection

The quantitative real-time PCR (Q-PCR) was performed in a 10-μl reaction mix containing *Taq*Man Copy Number Reference Assay RNaseP (Applied Biosystems, Foster City, CA) as the internal control. To determine the ratio of MCPyV DNA to MCPyV DNA from the reference MCC (MCC = 1.0) for each LCH case, Q-PCR was performed using an ABI PRISM 7900HT Sequence Detection System (Applied Biosystems). A total of 2 μL (~30 ng) of each DNA sample was amplified with 5 μL of EXPRESS qPCR Supermix with Premixed ROX (Invitrogen, Carlsbad, CA), 240 nmol/L of fluorescein-labeled locked nucleic acid hydrolysis probe 22 (5′-TGGTGGAG-3′) from a Universal Probe Library (Roche Diagnostics, Basel, Switzerland), and 0.9 μmol/L of a primer in a final volume of 10 μL. A primer pair targeting the position 859–934 on MCC350 (GenBank EU375803) [23] was used (MCPyV large T [LT]). The forward primer was 5′-AGGTTGACGAGGCCCCTAT-3′, and the reverse primer was 5′-TTCCCGAAGCT-GAATCCTC-3′ (amplicon size 76 bp). Locked nucleic acid probe 22 was used for MCPyV DNA detection. Thermal cycling consisted of incubation for 2 minutes at 50°C with an initial denaturation for 10 minutes at 95°C followed by 40 cycles of denaturation for 15 seconds at 95°C and annealing for 1 minute at 60°C, as previously described [23]. The ratio of the virus was determined using the signal in the positive MCC sample as a reference. Thresholds were plotted against each standard sample. All reactions of samples and controls were performed in triplicate, and the average is reported. The MCPyV DNA ratio in each sample was determined on the basis of the corresponding standard curves.

2.5. Immunohistochemistry for detection of MCPyV-LT

For the detection of MCPyV-LT antigen expression, IHC staining was performed using monoclonal antibody CM2B4 (mouse monoclonal IgG2b, 200 μg/mL; sc-136172; Santa Cruz Biotechnology, CA), which was generated using the peptide fragment of MCPyV-LT as an immunogen [23]. Four-micrometer LCH sample sections were deparaffinized and rehydrated. Endogenous peroxidase activity was blocked using 3% hydrogen peroxide in methanol for 15 minutes. Antigen retrieval was performed by incubating the sections in citrate buffer (pH 6.0) for 10 minutes at 95°C. The sections were incubated with CM2B4 (diluted at 1:100) overnight at 4°C and then washed in phosphate-buffered saline. Peroxidase-conjugated goat antimouse IgG was applied as the secondary antibody. Sections were incubated for 30 minutes at room temperature then washed in phosphate-buffered saline. Diaminobenzidine was used as the chromogen.

2.6. Statistical analysis

Comparisons of the values of the MCPyV DNA sequences from patients with LCH-RO+ and those with LCH-RO− were statistically analyzed using Fisher's exact test. The numbers of MCPyV DNA sequences obtained by

Q-PCR of patients with LCH, RLH, and non-LCH dermal disease data were also correlated using Fisher's exact test. Differences between the values were considered statistically significant at $P < .05$.

3. Results

3.1. MCPyV DNA in PBMCs from patients with LCH

The MCPyV DNA sequences were detected in PBMCs from patients with LCH-RO+ in 2 of the 3 analyzed samples, but there were no DNA sequences in any of the 12 samples corresponding to LCH-RO− ($P = .029$). Comparisons of MCPyV DNA sequences in PBMCs of patients with SS-LCH and of patients with MS-LCH did not differ significantly (0/6 versus 2/9; $P = .49$) (Table 1).

3.2. MCPyV DNA sequences in LCH tissues versus tissues of RLH, non-LCH skin diseases, and DLA

The viral loads of MCPyV detected by Q-PCR analysis in LCH tissues are shown in Table 2. MCPyV DNA sequences were detected in 12 of 13 tissue samples from patients with LCH, a significant difference from tissues from RLH patients (0/5; $P = .0007$; Table 3) or DLA patients (5/20; $P = .0007$; Table 4). The numbers of MCPyV DNA sequences in all four LCH tissues from patients younger than 2 years indicated a significant difference from tissues of non-LCH dermal disease patients of the same age (0/11; $P = .0007$), as reported in Tables 2 and 5.

Two tissue samples were obtained at 2 times from patient LCHT3 (Table 2) affected by an LCH lesion located in the epidural space between the fifth and seventh thoracic vertebrae. The MCPyV DNA was not detected in the first specimen that clearly contained LCH cells, whereas the second specimen obtained during a later second operation confirmed the presence of MCPyV DNA sequences. Comparatively, the two fragments obtained from patient LCHT7, the first from the femur and the second from the rib, both demonstrated the presence of MCPyV DNA sequences (Table 2).

3.3. MCPyV-DNA sequences in microdissected LCH lesions in comparison with microdissected DLA tissues

The microdissected areas containing S100-positive cells showed MCPyV DNA sequences by Q-PCR analysis in four of the five LCH samples (Table 6) and in both DLA samples (Table 7). Of note, MCPyV DNA sequences were not detected in LCH cells from patient LCHT12, although MCPyV DNA was detected in microdissected epidermis that included S100-positive LCs (viral load = 0.0006 copies/cell). Comparatively, the microdissected areas containing S100-negative lymphoid cells within the LCH or DLA tissues did not contain MCPyV DNA sequences in any of the 5 LCH samples or the two DLA samples analyzed.

3.4. IHC staining for MCPyV-LT

Positive cytoplasmic or nuclear immunoreactivity was observed in LCH cells corresponding to tissues where a higher viral load was detected by Q-PCR (2/13; LCHT7 and LCHT12; Fig.) compared with absent immunoreactivity in LCH tissues with low viral loads (see Table 2).

Table 1 Clinical characteristics and amounts of MCPyV-DNA in PBMCs of patients with Langerhans cell histiocytosis

Patient	Age/Sex	Subtype	Distribution	Risk organ	Viral load (Q-PCR)
LCHB1	0 mo/F	MS	Skin, BM	+	+ (0.0003)
LCHB2	3 mo/M	MS	Skin, thymus, oral mucosa, liver, BM, LN	+	+ (0.001)
LCHB3	1 y 4 mo/M	MS	Skin, liver, spleen, lung	+	−
LCHB4	1 y/M	MS	Bone, orbit	−	−
LCHB5	1 y 2 mo/F	MS	Skin, bone	−	−
LCHB6	1 y 4 mo/M	MS	Skin, bone	−	−
LCHB7	2 y/M	MS	Skin, LN	−	−
LCHB8	3 y/M	MS	Bone, LN	−	−
LCHB9	12 y/F	MS	Skin, CNS	−	−
LCHB10	3 mo/M	SS	Skin	−	−
LCHB11	1 y 7 mo/F	SS	Bone	−	−
LCHB12	2 y/M	SS	Bone	−	−
LCHB13	4 y/F	SS	Bone	−	−
LCHB14	6 y/M	SS	Bone	−	−
LCHB15	7 y/M	SS	Bone	−	−

NOTE. Median age of 15 patients was 1 y 7 mo (range 0 mo to 7 y). Viral load is shown as copies per cell in cases positive for MCPyV.
Abbreviations: BM, bone marrow; CNS, central nervous system; LCHB, Langerhans cell histiocytosis blood; LN, lymph node; MS, multisystem LCH; SS, single-system LCH; +, involvement of at least one high-risk organ or viral load detected; −, no involvement of high-risk organ or no viral load detected.

Table 2 Clinical characteristics and amounts of MCPyV in tissues of patients with Langerhans cell histiocytosis

Patient	Age/sex	Subtype	Risk organ	Biopsy site	Q-PCR (Viral Load)	MCPyV-LT (CM2B4)
LCHT1	86 y/F	SS	–	Bone	+ (0.006)	–
LCHT2	9 mo/F	SS	–	Oral mucosa	+ (0.002)	–
LCHT3	52 y/M	SS	–	Soft tissue	+ (0.002)	–
LCHT4	14 y/M	SS	–	Bone	+ (0.002)	–
LCHT5	5 mo/F	SS	–	Skin	+ (0.005)	–
LCHT6	41 y/F	SS	–	Pituitary	+ (0.002)	–
LCHT7	21 y/M	SS	–	Bone	+ (0.027)	+
LCHT8	6 y/F	MS	–	Bone	+ (0.006)	–
LCHT9	2 y/F	MS	–	Bone	–	–
LCHT10	7 y/F	MS	–	Soft tissue	+ (0.0001)	–
LCHT11	39 y/F	MS	–	Skin	+ (0.002)	–
LCHT12	1 y/F	MS	+	Skin	+ (0.033)	+
LCHT13	6 mo/F	MS	–	Skin	+ (0.003)	–

NOTE. Median age of SS-LCH patients (n = 7) was 22 y (range, 5 mo to 86 y). Median age of MS-LCH patients (n = 6) was 4 y (range, 6 mo to 39 y). Abbreviations: CM2B4, immunostaining of MCPyV large T antigen in LCH cells; LCHT, Langerhans cell histiocytosis tissue; MS, multisystem LCH; SS, single-system LCH; +, involvement of at least one high-risk organ or viral load detected; –, no involvement of high-risk organ or no viral load detected.

4. Discussion

Our previous data indicated that Q-PCR was the most sensitive method for the detection of MCPyV, superior to single PCR and immunohistochemistry staining [19,23]. The Q-PCR for MCPyV-LT also was more sensitive than immunohistochemistry using the CM2B4 antibody (see Table 2). In this report, we describe the presence of MCPyV DNA sequences in two blood samples (see Table 1) as well as in four LCH tissues samples obtained from children younger than 2 years (Table 2). The viral DNA load in blood samples ranged from 30 to 100 molecules per 100 000 cells (0.0003 to 0.001 per cell). No significant differences in the numbers of MCPyV DNA sequences were observed between patients with SS-LCH and those with MS-LCH (Table 1). Concerning the LCH tissues, MCPyV DNA sequences were detected in microdissected areas containing S100-immunoreactive cells in four of the five LCH samples and in both analyzed DLA samples. In contrast, the microdissected areas containing lymphoid cells non-reactive with the anti-S100 antibody did not show MCPyV DNA sequences. Remarkably, a viral DNA load of 0.0006 copies/cell was detected in microdissected areas of the epidermal layer, which contained S100-positive LCs (see Table 6, patient LCHT12).

MCPyV was frequently detected in the skin of healthy individuals [19,21]. Surprisingly, buffy coats of healthy adult blood donors, which were examined for MCPyV DNA tag sequences, showed a prevalence of 22%, with viral loads ranging from 10 to 100 molecules per 100 000 cells (0.0001 to 0.001 per cell) [26]. As LCs capture foreign antigens in the epidermal layer and migrate toward the lymph nodes,

Table 3 Clinical characteristics and MCPyV in tissues of patients with RLH

Patient	Age (y)/sex	Biopsy site	Q-PCR
RLH1	72/F	Lung	–
RLH2	79/F	Lung	–
RLH3	62/M	Nasal cavity	–
RLH4	32/F	Lymph node	–
RLH5	75/F	Lymph node	–

NOTE. Median age of patients (n = 5) was 72 y (range, 32-79 y).

Table 4 Clinical characteristics and lesional MCPyV data of patients with DLA

Patient	Age (y)/sex	Q-PCR (Viral load)
DLA1	66/F	+ (0.002)
DLA2	54/M	–
DLA3	81/M	+ (0.004)
DLA4	58/M	+ (0.001)
DLA5	63/M	+ (0.001)
DLA6	79/F	+ (0.006)
DLA7	66/M	–
DLA8	65/F	–
DLA9	86/M	–
DLA10	74/M	–
DLA11	35/M	–
DLA12	30/F	–
DLA13	72/F	–
DLA14	87/M	–
DLA15	39/M	–
DLA16	81/M	–
DLA17	73/M	–
DLA18	43/M	–
DLA19	39/M	–
DLA20	68/M	–

NOTE. All biopsies were of lymph nodes. Median age of patients (n = 20) was 66 y (range, 30-87 y).

Table 5 Clinical characteristics and lesional MCPyV data of patients younger than 2 years with non-LCH dermal diseases

Patient	Age/sex	Diagnosis	Q-PCR
S1	1 y 4 mo/F	Nevocellular nevus	–
S2	1 y 6 mo/F	Nevocellular nevus	–
S3	8 mo/F	Xanthogranuloma	–
S4	1 y 6 mo/F	Dermoid cyst	–
S5	1 y 9 mo/M	Blue nevus	–
S6	1 mo/F	Nevocellular nevus	–
S7	1 y 3 mo/F	Nevus sebaceous	–
S8	1 mo/F	Xanthogranuloma	–
S9	1 y 4 mo/F	Dermoid cyst	–
S10	1 y 3 mo/F	Dermatitis	–
S11	1 y 4 mo/F	Nevocellular nevus	–

NOTE. All biopsies were from skin. Median age of patients (n = 11) was 1 y 4 mo (range, 1 mo to 1 y 9 mo).

detection of MCPyV DNA sequences in both whole (25%; see Table 4) and microdissected DLA tissues (Table 7) suggest that LCs behave as a reservoir for MCPyV in an asymptomatic state and that LCs can transfer the MCPyV DNA from the epidermal layer to lymph nodes.

In patients affected by LCH, antibodies against MCPyV viral proteins (VP) were not detected by enzyme-linked immunoassay in patients younger than 2 years, compared with an incidence of 40% in patients 2 to 5 years of age, about 50% in patients 6–50 years, and 80% in patients older than 50 years [27]. Conversely, in a large seroepidemiologic study, Kean and coworkers [28] showed that about 20% (1–5 years old), 30% (6–10 years), 40% (11–70 years), and 60% (above 70 years) of the healthy population carries anti-MCPyV VP-1 antibodies. Although LCs seem to provide a sanctuary for MCPyV instead of inducing host resistance, as happens with several viruses [16,29], virtually transformed LCH cells may produce intense tissue overreaction and symptoms.

Considering our data, ie, the presence of MCPyV DNA in 4 samples of LCH tissue in patients younger than 2 years (Table 2) together with the previously published seroprevalence of MCPyV in a both healthy population between 1 and 5 years of age [28] and LCH patients younger than 2 years [27] and the absence of viral sequences in non-LCH skin lesions (Table 5), the primary infection with MCPyV may play a significant pathogenic role in LCH. Thus, the primary infection with MCPyV at the onset of LCH might be related to a disease with severe progression in comparison with a milder course of the disease with onset in the carrier state.

Table 7 Detection of MCPyV DNA by Q-PCR in whole DLA samples and microdissected S100+ or S100– DLA lesions

Patient	Q-PCR (viral load)	Q-PCR (Microdissection)	
		S100+ (viral load)	S100–
DLA3	+ (0.004)	+ (0.0003)	–
DLA4	+ (0.001)	+ (0.001)	–

With respect to the presence of other pathogenic infectious agents, Epstein-Barr virus [30], human cytomegalovirus [31], and human herpesvirus 6 [32] have been found in patients affected by LCH. However, at present, they are regarded as bystanders in LCH lesions according to case-controlled seroepidemiologic studies and in situ hybridization analysis [16,33]. In this regard, our data suggest the presence of MCPyV in LCH tissue lesions, especially in patients younger than 2 years (100%; Table 2), excluding the occasional viral infection. In this context, the presence of MCPyV DNA was reported in the blood of a 53-year-old recipient of a renal allograft and a 75-year-old patient with chronic psoriasis and MCC [34]. Mertz and colleagues [34] reported that CD14+ activated monocytes might be a reservoir of MCPyV in the blood and that these cells can spread the inflammatory reactions to various locations in the body. Presumably, LCH cells that currently show elevated numbers of CD14 molecules may also disseminate granulomatous lesions in patients affected by LCH with high-risk organ involvement [35].

5. Conclusion

This is to our knowledge the first report of a relation between MCPyV infection and LCH. We suggest that MCPyV triggers an inflammatory process associated with LCH activity and subtype. The frequent but lower viral loads

Table 6 Detection of MCPyV-DNA by Q-PCR of whole LCHT samples and microdissected S100+ or S100– from LCH lesions

Patient	Subtype	Biopsy site	Viral load (Q-PCR)	Q-PCR (Microdissection)	
				S100+ (Viral load)	S100–
LCHT1	SS	Bone	+ (0.006)	+ (0.02)	–
LCHT3	SS	Soft tissue	+ (0.002)	+ (0.0006)	–
LCHT10	MS	Soft tissue	ND	+ (0.0001)	–
LCHT12	MS	Skin	+ (0.033)[a]	–	(+)
LCHT13	MS	Skin	+ (0.003)	+ (0.001)	–

NOTE. MCPyV-DNA was detected in microdissected epidermal layers, which included S100-positive Langerhans cells (viral load 0.0006).
Abbreviations: MS, multisystem LCH; ND, not done; SS, single-system LCH.

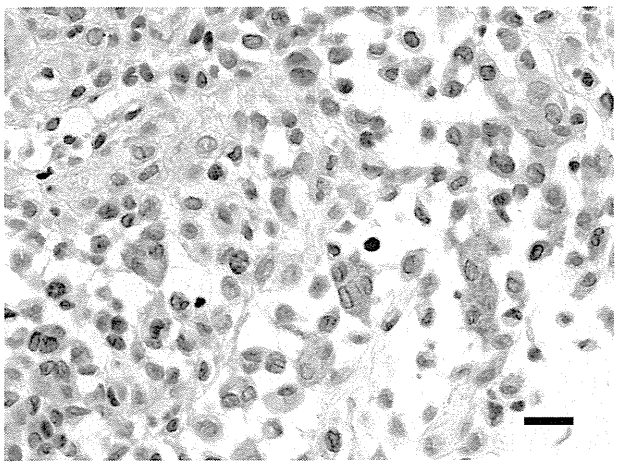

Fig. Immunoreactivity for Merkel cell polyoma virus large T-antigen using monoclonal antibody CM2B4 in multisystem Langerhans cell histiocytosis tissue (LCHT7). Scale bar, 20 μm.

detected by Q-PCR and low positive immunoreactivity rate using the anti-MCPyV-LT antibody in 2 of 13 of LCH tissue samples suggest that development of LCH is more a reactive rather than a neoplastic process, which may be relevant to MCPyV infection. We propose that LCH subtypes are defined by abnormal immunoreactivity against the MCPyV pathogen with an underlying oncogenic capacity. These data open novel possibilities for using antiviral molecules for therapeutic interventions in patients affected by LCH.

Acknowledgment

The authors thank all patients, parents, and physicians who participated in this study.

References

[1] Willman CL, Busque L, Griffith BB, et al. Langerhans'-cell histiocytosis (histiocytosis X)—a clonal proliferative disease. N Engl J Med 1994;331:154-60.
[2] Yu RC, Chu C, Buluwela L, Chu AC. Clonal proliferation of Langerhans cells in Langerhans cell histiocytosis. Lancet 1994;343:767-8.
[3] Badalian-Very G, Vergilio JA, Degar BA, et al. Recurrent *BRAF* mutations in Langerhans cell histiocytosis. Blood 2010;116:1919-23.
[4] Donadieu J, Egeler RM, Pritchard J. Langerhans cell histiocytosis: a clinical update. In: Weitzman S, Egeler RM, editors. Histiocytic Disorders of Children and Adults. Cambridge, UK: Cambridge University Press; 2005. p. 95-129.
[5] Hamre M, Hedberg J, Buckley J, et al. Langerhans cell histiocytosis: an exploratory epidemiologic study of 177 cases. Med Pediatr Oncol 1997;28:92-7.
[6] Finn LS, Jaffe R. Langerhans' cell granuloma confined to the bile duct. Pediatr Pathol Lab Med 1997;17:461-8.
[7] Kaplan KJ, Goodman ZD, Ishak KG. Liver involvement in Langerhans' cell histiocytosis: a study of nine cases. Mod Pathol 1999;12:370-8.
[8] Coury F, Annels N, Rivollier A, et al. Langerhans cell histiocytosis reveals a new IL-17A-dependent pathway of dendritic cell fusion. Nat Med 2008;14:81-7.
[9] Allen CE, McClain KL. Interleukin-17A is not expressed by CD207(+) cells in Langerhans cell histiocytosis lesions. Nat Med 2009;15:483-4 [author reply 4–5].
[10] Peters TL, McClain KL, Allen CE. Neither IL-17A mRNA nor IL-17A protein are detectable in Langerhans cell histiocytosis lesions. Mol Ther 2011;19:1433-9.
[11] Murakami I, Morimoto A, Oka T, et al. IL-17A receptor expression differs between subclasses of Langerhans cell histiocytosis, which might settle the IL-17A controversy. Virchows Arch 2013;462: 219-28.
[12] Ryzhakov G, Lai CC, Blazek K, To KW, Hussell T, Udalova I. IL-17 boosts proinflammatory outcome of antiviral response in human cells. J Immunol 2011;187:5357-62.
[13] Ryzhakov G, Blazek K, Lai CC, Udalova IA. IL-17 receptor adaptor protein Act1/CIKS plays an evolutionarily conserved role in antiviral signaling. J Immunol 2012;189:4852-8.
[14] Murakami I, Oka T, Kuwamoto S, et al. Tyrosine phosphatase SHP-1 is expressed higher in multisystem than in single-system Langerhans cell histiocytosis by immunohistochemistry. Virchows Arch 2011;459: 227-34.
[15] An H, Hou J, Zhou J, et al. Phosphatase SHP-1 promotes TLR- and RIG-I-activated production of type I interferon by inhibiting the kinase IRAK1. Nat Immunol 2008;9:542-50.
[16] da Costa CET, Annels NE, Egeler RM. The immunological basis of Langerhans cell histiocytosis. In: Weitzman S, Egeler RM, editors. Histiocytic Disorders of Children and Adults. Cambridge, UK: Cambridge University Press; 2005. p. 66-82.
[17] Garabedian L, Struyf S, Opdenakker G, Sozzani S, Van Damme J, Laureys G. Langerhans cell histiocytosis: a cytokine/chemokine-mediated disorder? Eur Cytokine Netw 2011;22:148-53.
[18] Cyster JG. Chemokines and the homing of dendritic cells to the T cell areas of lymphoid organs. J Exp Med 1999;189:447-50.
[19] Matsushita M, Kuwamoto S, Iwasaki T, et al. Detection of Merkel cell polyomavirus in the human tissues from 41 Japanese autopsy cases using polymerase chain reaction. Intervirology 2013;56:1-5.
[20] Tolstov YL, Knauer A, Chen JG, et al. Asymptomatic primary Merkel cell polyomavirus infection among adults. Emerg Infect Dis 2011;17: 1371-80.
[21] Foulongne V, Kluger N, Dereure O, et al. Merkel cell polyomavirus in cutaneous swabs. Emerg Infect Dis 2010;16:685-7.
[22] Feng H, Shuda M, Chang Y, Moore PS. Clonal integration of a polyomavirus in human Merkel cell carcinoma. Science 2008;319: 1096-100.
[23] Kuwamoto S. Recent advances in the biology of Merkel cell carcinoma. Hum Pathol 2011;42:1063-77.
[24] Kubo A, Nagao K, Yokouchi M, Sasaki H, Amagai M. External antigen uptake by Langerhans cells with reorganization of epidermal tight junction barriers. J Exp Med 2009;206:2937-46.
[25] Jaffe R, Weiss LM, Facchetti F. Tumours derived from Langerhans cells. In: Swerdlow SH, Campo E, Harris NL, et al, editors. WHO Classification of Tumours of Haematopoietic and Lymphoid Tissues. Lyon, France: IARC; 2008. p. 358-60.
[26] Pancaldi C, Corazzari V, Maniero S, et al. Merkel cell polyomavirus DNA sequences in the buffy coats of healthy blood donors. Blood 2011;117:7099-101.
[27] Tolstov YL, Pastrana DV, Feng H, et al. Human Merkel cell polyomavirus infection II: MCV is a common human infection that can be detected by conformational capsid epitope immunoassays. Int J Cancer 2009;125:1250-6.
[28] Kean JM, Rao S, Wang M, Garcea RL. Seroepidemiology of human polyomaviruses. PLoS Pathog 2009;5:e1000363.
[29] Banchereau J, Steinman RM. Dendritic cells and the control of immunity. Nature 1998;392:245-52.

[30] Shimakage M, Sasagawa T, Kimura M, et al. Expression of Epstein-Barr virus in Langerhans' cell histiocytosis. HUM PATHOL 2004;35: 862-8.
[31] Kawakubo Y, Kishimoto H, Sato Y, et al. Human cytomegalovirus infection in foci of Langerhans cell histiocytosis. Virchows Arch 1999;434:109-15.
[32] Leahy MA, Krejci SM, Friednash M, et al. Human herpesvirus 6 is present in lesions of Langerhans cell histiocytosis. J Invest Dermatol 1993;101:642-5.
[33] Jeziorski E, Senechal B, Molina TJ, et al. Herpes-virus infection in patients with Langerhans cell histiocytosis: a case-controlled sero-epidemiological study, and in situ analysis. PLoS One 2008;3:e3262.
[34] Mertz KD, Junt T, Schmid M, Pfaltz M, Kempf W. Inflammatory monocytes are a reservoir for Merkel cell polyomavirus. J Invest Dermatol 2010;130:1146-51.
[35] Geissmann F, Lepelletier Y, Fraitag S, et al. Differentiation of Langerhans cells in Langerhans cell histiocytosis. Blood 2001;97: 1241-8.

ARTICLE

Journal of Cellular Biochemistry 115:585–595 (2014)

Journal of Cellular Biochemistry

Osteopontin Has a Crucial Role in Osteoclast-Like Multinucleated Giant Cell Formation

Yukiko Oh,[1]* Iekuni Oh,[2] Junko Morimoto,[3] Toshimitsu Uede,[3] and Akira Morimoto[1]

[1]*Department of Pediatrics, Jichi Medical University School of Medicine, 3311-1, Yakushi-ji, Shimotsuke, Tochigi 329-0498, Japan*

[2]*Department of Hematology, Jichi Medical University School of Medicine, 3311-1, Yakushi-ji, Shimotsuke, Tochigi 329-0498, Japan*

[3]*Division of Molecular Immunology, Institute for Genetic Medicine, Hokkaido University, Kita-15, Nishi-7, Kita-ku, Sapporo 060-0815, Japan*

ABSTRACT

The osteoclast (OC) is a major player in the pathogenic bone destruction of inflammatory bone diseases such as rheumatoid arthritis and Langerhans cell histiocytosis. Recently, it was shown that immature dendritic cells (iDC) fuse faster and more efficiently than monocytes in forming OC-like multinucleated giant cells (MGCs), and that osteopontin (OPN) is involved in the pathogenesis of inflammatory bone diseases. In this study, we hypothesized that OPN is a key factor for generation of OC-like MGCs from iDCs. We used an in vitro culture system to differentiate iDCs, derived from monocytes obtained from the blood of healthy donors, into OC-like MGCs. We evaluated OPN levels and expression of OPN receptors during the course of differentiation. OPN has an arginine-glycine-aspartic acid (RGD) motif, and protease cleavage reveals a SVVYGLR motif. The concentrations of both full-length and cleaved forms of OPN increased during the course of OC-like MGC formation. Expression of OPN RGD- and SVVYGLR-recognizing receptors also increased at later stages. We analyzed whether blocking OPN binding to its receptors affected OC-like MGC formation. Monocytes treated with OPN siRNA were able to differentiate into iDCs effectively; however, differentiation of these iDCs into OC-like MGCs was significantly reduced. The formation of OC-like MGCs was not significantly reduced by RGD synthetic peptide. By contrast, SVVYGLR synthetic peptide caused a significant reduction. These data suggest that the cleaved form of OPN plays a critical role in driving iDC differentiation into OC-like MGCs in the early phase of differentiation, in an autocrine and/or paracrine fashion. J. Cell. Biochem. 115: 585–595, 2014.

KEY WORDS: OSTEOPONTIN; OSTEOCLAST; IMMATURE DENDRITIC CELL; MULTINUCLEATED GIANT CELL; INFLAMMATORY BONE DISEASE

Osteoclasts (OC) are bone-resorbing giant polykaryon cells that differentiate from mononuclear macrophage/monocyte-lineage hematopoietic precursors. Upon stimulation by cytokines, such as macrophage colony-stimulating factor (M-CSF) and receptor activator of NF-κB ligand (RANKL), OC precursor cells migrate and attach onto the bone surface. There they fuse with each other to form multinucleated giant cells (MGCs) and mediate bone resorption [Teitelbaum, 2000].

Osteopontin (OPN) plays an important role physiologically in bone remodeling, especially in bone resorption, by modulating OC function [Chellaiah et al., 2003; Standal et al., 2004]. OPN contains the classical cell-binding motif arginine-glycine-aspartic acid (RGD) that binds cell surface RGD-recognizing integrins such as αvβ1, αvβ3, α5β1, and CD44 variant (v) 6 [Hu et al., 1995; Gao et al., 2003]. RGD-recognizing integrins are expressed by a variety of cells including fibroblasts, smooth muscle cells, endothelial cells, epithelial cells, and immune cells [Uede, 2011]. OPN can be cleaved by proteases, including thrombin and plasmin, which exposes a serine-valine-valine-tyrosine-glycine-leucine-arginine (SVVYGLR) motif [Yokosaki et al., 1999]. This motif is recognized by non-RGD-recognizing integrins such as α4β1 expressed by T cells and macrophages, and α9β1 expressed by fibroblasts, neutrophils, macrophages, smooth muscle cells, and OCs [Smith et al., 1996; Green et al., 2001].

Grant sponsor: The Ministry of Health, Labor and Welfare, Japan; Grant sponsor: Japan Society for Promotion of Science (JSPS); Grant sponsor: Jichi Medical University Graduate Student Start-Up Grant for Young Investigators; Grant number: 22591167; Grant sponsor: Grant-in-Aid for Scientific Research (KAKENHI) from the Ministry of Education, Culture, Sports, Science and Technology, Japan; Grant sponsor: JKA Foundation.

*Correspondence to: Yukiko Oh, MD, Department of Pediatrics, Jichi Medical University School of Medicine, 3311-1, Yakushi-ji, Shimotsuke, Tochigi 329-0498, Japan. E-mail: yukikok@jichi.ac.jp

Manuscript Received: 16 May 2013; Manuscript Accepted: 10 October 2013

Accepted manuscript online in Wiley Online Library (wileyonlinelibrary.com): 15 October 2013

DOI 10.1002/jcb.24695 • © 2013 Wiley Periodicals, Inc.

OCs play a major role in the pathogenic bone destruction of rheumatoid arthritis (RA) and Langerhans cell histiocytosis (LCH) [Redlich et al., 2002; da Costa et al., 2005]. Recently, it was revealed that immature dendritic cells (iDC) fuse more quickly and efficiently than monocytes to form OC-like MGCs in the inflammatory environment [Rivollier et al., 2004]. This suggests that iDC-derived OCs may be directly involved in the osteolytic lesions observed in inflammatory bone diseases such as RA or LCH. OPN is implicated in the pathogenesis of RA [Yumoto et al., 2002; Yamamoto et al., 2007] and LCH [Prasse et al., 2009; Allen et al., 2010].

Based on these findings, we hypothesized that OPN is a key factor in the formation of OC-like MGCs from iDCs. In this study we found that OPN, particularly after cleavage, plays a critical role in the formation of OC-like MGCs from iDCs in an autocrine and paracrine manner.

MATERIALS AND METHODS

MONOCYTE PURIFICATION AND IDC DIFFERENTIATION

Monocytes and iDCs were defined by the expression of CD14 and CD1a, respectively [Chapuis et al., 1997]. PBMC were obtained from healthy adult volunteer donors. Informed consent was obtained from them. The ethics committee, Jichi Medical University School of Medicine approved this study. A positive selection of $CD14^+$ cells was performed by adding MACS colloidal superparamagnetic microbeads conjugated with monoclonal anti-human CD14 Abs (IgG2a), (Miltenyi Biotec, Tokyo, Japan) to freshly prepared PBMC preparation in MACS buffer according to the manufacture's instructions. Briefly, after incubation of cells and microbeads (15 min at 4°C), cells were washed with MACS buffer, resuspended, and loaded onto the top of the separation column. Trapped $CD14^+$ PBMC were eluted with a sixfold amount of cold MACS buffer. Using flow cytometry, the purity of the $CD14^+$ cells was evaluated at $98.8 \pm 0.4\%$.

Purified monocytes were used to generate monocyte-derived iDCs in vitro, as previously described [Rivollier et al., 2004]. Briefly, monocytes were seeded at 10^6 cells/ml and maintained in RPMI 1640 (Life Technologies, Paisley, UK) supplemented with 10 mM N-2-hydroxyethylpiperazine-N′-2-ethanesulfonic acid (HEPES), 2 mM L-glutamine, 100 U/ml penicillin and 100 μg/ml streptomycin (Life Technologies), 10% heat-inactivated fetal calf serum (FCS; Biological Industries, Beit Haemek, Israel), 50 ng/ml human recombinant (h) granulocyte-macrophage colony-stimulating factor (GM-CSF), and 500 U/ml h IL-4 (PeproTech, Rocky Hill, NJ). After 5 days in culture, more than 90% of the cells were iDCs as assessed by CD1a labeling.

OC-LIKE MGC FORMATION AND TRAP ASSAY

iDCs were seeded at 1,600 cells/mm^2 in 48-well plates, into which a sterilized glass coverslip was placed, in α-minimum essential medium (α-MEM) (Life Technologies) supplemented with 10% FCS, 2 mM L-glutamine, 100 U/ml penicillin, and 100 μg/ml streptomycin in the presence of 25 ng/ml M-CSF and 100 ng/ml RANKL (PeproTech, Rocky Hill, NJ). During the course of differentiation, we harvested culture supernatants and various cells including monocytes, iDCs, and various differential stages of OC-like MGCs at day 4 (OC4), day 8 (OC8), and day 12 (OC12). Tartrate-resistant acid phosphatase (TRAP) activity, a signature marker for OCs, was assessed using a leukocyte acid phosphatase kit (Sigma–Aldrich) at day 12. Nuclear DNA was stained with 10 μg/ml Hoechst 33342 (Sigma–Aldrich) for 30 min at 37°C and fixed with 15% formol.

SUPPRESSION OF OPN BY RNA INTERFERENCE

Suppression of OPN expression was performed by RNA interference using specific small interfering RNA oligonucleotides (siRNA) (ccaaguaaguccaacgaaaTT). Control siRNA sequence was acucuaucugcacgcugacTT. siRNAs were transfected into human monocytes or monocyte-derived iDCs using Lipofectamine RNAiMAX (Life Technologies). Transfected monocytes or iDCs were cultured to form OC-like MGCs as described above. The number of OC-like MGCs (TRAP-positive and strictly more than two nuclei) was counted on day 7 of OC differentiation.

INHIBITION OF MGC FORMATION WITH SYNTHETIC PEPTIDES DERIVED OPN INTERNAL SEQUENCE

In order to examine whether the interaction of OPN and its receptors is involved in MGC formation, we used synthetic peptides (RGD and SVVYGLR) to both RGD-recognizing and SVVYGLR-recognizing integrins. RGD and SVVYGLR peptides interfere with the binding of OPN to RGD- and non RGD ($\alpha4\beta1$ and $\alpha9\beta1$) integrins, respectively [Storgard et al., 1999; Green et al., 2001]. MGCs were differentiated from iDCs, in the presence of 10 μg/ml RGD or RGE (control) peptides (Abbiotec, San Diego, CA), or 1 μg/ml SVVYGLR or GRVLYSV (control) peptides (GenScript, Piscataway, NJ). The number of OC-like MGCs (TRAP-positive and strictly more than two nuclei) was counted on day 7 of OC differentiation.

IMMUNOFLUORESCENCE AND MICROSCOPY

Monocytes and iDC were attached to slide glass by cytospin. Monocytes, iDC and cells cultured on glass coverslips (OC4, OC8, OC12) were first fixed with 4% paraformaldehyde for 30 min at 4°C. The slide glass or the glass coverslips were incubated in normal goat serum for 30 min at 30°C, followed by primary antibody (polyclonal rabbit anti-human OPN antibody (IgG), (Abcam, Cambridge, UK), polyclonal rabbit anti-human CD1a antibody (Sigma–Aldrich, St. Louis, MO), monoclonal mouse anti-human CD44v6 antibody (IgG1), (Leica, Newcastle upon Tyne, UK), monoclonal mouse anti-human $\alpha v\beta3$ antibody (IgG1), (Hycult Biotech, Uden, The Netherlands), and monoclonal mouse anti-human $\alpha9\beta1$ antibody (IgG1), (Abcam) for a further overnight at room temperature. Rabbit IgG (SP137), (Abcam) and mouse IgG1 (MOPC21), (Affinity BioReagents, Golden, CO) was used as substitute isotype control. After washing with PBS, the appropriate secondary antibody (Alexa Fluor 488 goat anti-mouse IgG (H + L), Alexa Fluor 488 goat anti-rabbit IgG (H + L), or Alexa Fluor 555 goat anti-mouse IgG (H + L) (Molecular Probes, Inc., Eugene, OR) was applied for 30 min at 30°C. Nuclear DNA was stained by DAPI (4′-6-diamidino-2-phenylindole). The cells were analyzed using an Olympus AX80 microscope equipped with an 40×/0.85 NA or a 100×/1.35 oil iris NA objective lens, an Olympus DP70 camera, and Olympus DP controller software (Olympus Co. Ltd., Tokyo, Japan). The number of CD1a positive cells and $\alpha9\beta1$ positive cells was counted on monocyte, iDC, and day 4, 8, 12 of OC differentiation.

QUANTIFICATION OF IMMUNOFLUORESCENCE

Images collected using the Olympus DP controller software were analyzed for immunofluorescence intensity using Adobe Photoshop Elements, version 11 (Adobe Systems Incorporated, Tokyo, Japan) as follows. Using the magic wand tool in the "Select" menu of Photoshop, the cursor was placed on α9β1-positive cytoplasm. The tolerance level of the magic wand tool was adjusted so that the entire positive cytoplasm was selected automatically. The mean staining intensity was calculated as follows: intensity score (IS) = mean of brightness of selected cells' red channel score (in arbitrary units, AU) using Adobe Photoshop Elements, version 11 [Murakami et al., 2013].

RELATIVE QUANTITATIVE RT-PCR

Levels of OPN, CD44v6, integrin αv, and integrin α9 mRNA were measured by relative quantitative real-time reverse transcription polymerase chain reaction (RT-PCR) using the 7500 Fast System (Applied Biosystems, Foster City, CA); β-actin was used as an internal standard. Briefly, RNA was isolated from the harvested cells using an RNeasy kit (Qiagen, Hilden, Germany), reverse transcribed, and PCR amplified using a One Step PrimeScript RT-PCR Kit (Takara Bio, Shiga, Japan), with TaqMan Gene Expression Assay primers for human OPN (Hs00959010), integrin αv (Hs00233808), integrin α9 (Hs00979865), CD44v6 (Hs01075854), and β-actin (Hs99999903). Data were analyzed using the $2^{-\Delta\Delta C_t}$ method.

MEASUREMENTS OF THE FULL-LENGTH AND THE CLEAVED FORMS OF OPN IN THE CELL SUPERNATANT

We measured the amounts of the full-length OPN in the cell culture supernatant with human osteopontin ELISA kit (R&D Systems, Minneapolis, MN) and the cleaved forms of OPN with human osteopontin N-half assay kit (IBL, Gunma, Japan), which can specifically measure the N-terminal OPN fragment cleaved by thrombin. N-terminal OPN fragments expose a cryptic epitope, SVVYGLR, which is recognized by α9β1 integrin. Thus, the presence of high amounts of N-half OPN indicates the involvement of α9β1 integrin in OC-like MGC differentiation.

FLOW CYTOMETRIC ANALYSIS

We used directly conjugated antibodies, FITC-anti-CD14 (M5E2), PE-anti-CD1a (HI149), FITC-IgG2a (G155-178), and PE-IgG1 (MOPC-21) (BD Pharmingen, Tokyo, Japan). Cells were suspended in PBS supplemented with 10% FCS (FACS buffer) and stained with appropriate concentrations of antibodies for 15 min on ice, then washed with FACS buffer. Cells were analyzed using a BD LSR cytometer and CellQuest software (BD, Tokyo, Japan).

DETERMINATION OF VIABILITY AND APOPTOSIS

For floating cells, we analyzed the proportion of viable and apoptotic cells using flow cytometry. The number of floating cells was counted, cells were suspended in binding buffer (BD Pharmingen, Tokyo, Japan), and cell suspensions were incubated with Annexin V-PE and 7-AAD (BD Pharmingen, Tokyo, Japan) for 15 min at room temperature. Cells were analyzed using a BD LSR Fortessa cell analyzer and FlowJo software (Tree Star, San Carlos, CA). Unstained cells were used as negative controls. Viable cells were defined as double negative for Annexin V and 7-AAD, and apoptotic cells were defined as Annexin V positive and 7-AAD negative. For analysis of adherent cells, cells cultured on glass coverslips were stained by 0.4% trypan blue to count viable cells. To detect apoptotic cells, terminal deoxynucleotidyl transferase mediated dUTP nick end labeling (TUNEL) stain was performed. Cells were fixed with 4% paraformaldehyde for 30 min at 4°C. The glass coverslips were incubated with permeabilization buffer for 2 min at 4°C, followed by FITC-labeled terminal deoxynucleotidyl transferase (TdT) enzyme for 90 min at 37°C. DNA was stained by DAPI. The cells were analyzed using an Olympus AX80 microscope.

QUANTIFICATION OF CASPASE-3 ACTIVITY

Caspase-3 activity was quantified using an ApoAlert Caspase-3 colorimetric assay kit (Clontech, Tokyo, Japan). This assay uses the spectrophotometric detection of the chromophore p-nitroaniline (pNA) after its cleavage by caspases from the labeled caspase-specific substrates. 1.5×10^5 cells were harvested at each stage (OC1, OC3, and OC7), and resuspended in 50 μl of lysis buffer and incubated for 10 min at 4°C. Cell suspension were centrifuged at 15,000 rpm for 10 min. Twenty-five microliters of the supernatants were added to 25 μl of 2× reaction buffer, and then incubated with caspase-3 substrate, aspartic acid-glutamic acid-valine-aspartic acid (DEVD)-p-nitroaniline (pNA), for 60 min at 37°C. The chromophore pNA was measured at 405 nm in Benchmark Plus microplate reader (BIO-RAD, Tokyo, Japan). We constructed a standard curve for each assay run using pNA in the concentration range of 0–200 μM, and converted optical density of each sample into pNA concentration.

MEASUREMENT OF INTRACELLULAR REACTIVE OXYGEN SPECIES PRODUCTION

Reactive oxygen species (ROS) activity was quantified using an OxiSelect Intracellular ROS assay kit (Cell Biolabs, San Diego, CA). Briefly, 1.5×10^5 cells were harvested at each differentiation stage (Mo, iDC, OC1, OC3, and OC7), and then incubated with 100 μl of 2′, 7′-dichlorodihydrofluorescin diacetate (DCFH-DA) at 37°C for 60 min. Cells were washed twice with PBS, and lysed by cell lysis buffer. Fluorescence was measured at 480 nm excitation/530 nm emission in Wallac 1420 ARVO MX (Perkin Elmer, Yokohama, Japan). We constructed a standard curve for each assay run using 2′, 7′-dichlorodihydrofluorescein (DCF) in the concentration range of 0–10 μM, and converted fluorescence intensity into DCF concentration.

INHIBITION OF ROS GENERATION

We used diphenyleneiodonium chloride (DPI) (Enzo Life Sciences, Lausen, Switzerland) or *N*-acetyl-L-cysteine (NAC) (Sigma–Aldrich) as ROS inhibitors. DPI was dissolved in Dimethyl sulfoxide (DMSO). NAC was dissolved in α-MEM, and pH was adjusted to 7.4 by the addition of NaOH. Monocytes or iDCs were incubated with 100 nM DPI or 20 mM NAC for 60 min at 37°C, and washed twice with medium. Pretreated monocytes were cultured with GM-CSF and IL-4 for 5 days, and pretreated iDCs were cultured with M-CSF and RANKL for 7 days.

STATISTICAL ANALYSIS

The paired *t*-test was used to analyze the difference between groups; $P < 0.05$ was considered significant. All error bars in this study represent the standard error mean of the mean (SEM). Statistical analyses were performed using Microsoft Excel software.

RESULTS

OPN PRODUCTION IS INCREASED DURING THE COURSE OF OC-LIKE MGC FORMATION FROM iDCs

The production of OPN mRNA and protein was investigated over the course of OC-like MGC formation from iDCs in vitro. First, we obtained monocytes from the blood of healthy adult volunteer donors and from them generated iDCs and then OC-like MGCs using an in vitro culture system (Fig. 1A). During the course of differentiation, we harvested culture supernatants and various cells including monocytes, iDCs, and various differential stages of OC-like MGCs at day 4 (OC4), day 8 (OC8), and day 12 (OC12). Monocytes had no detectable

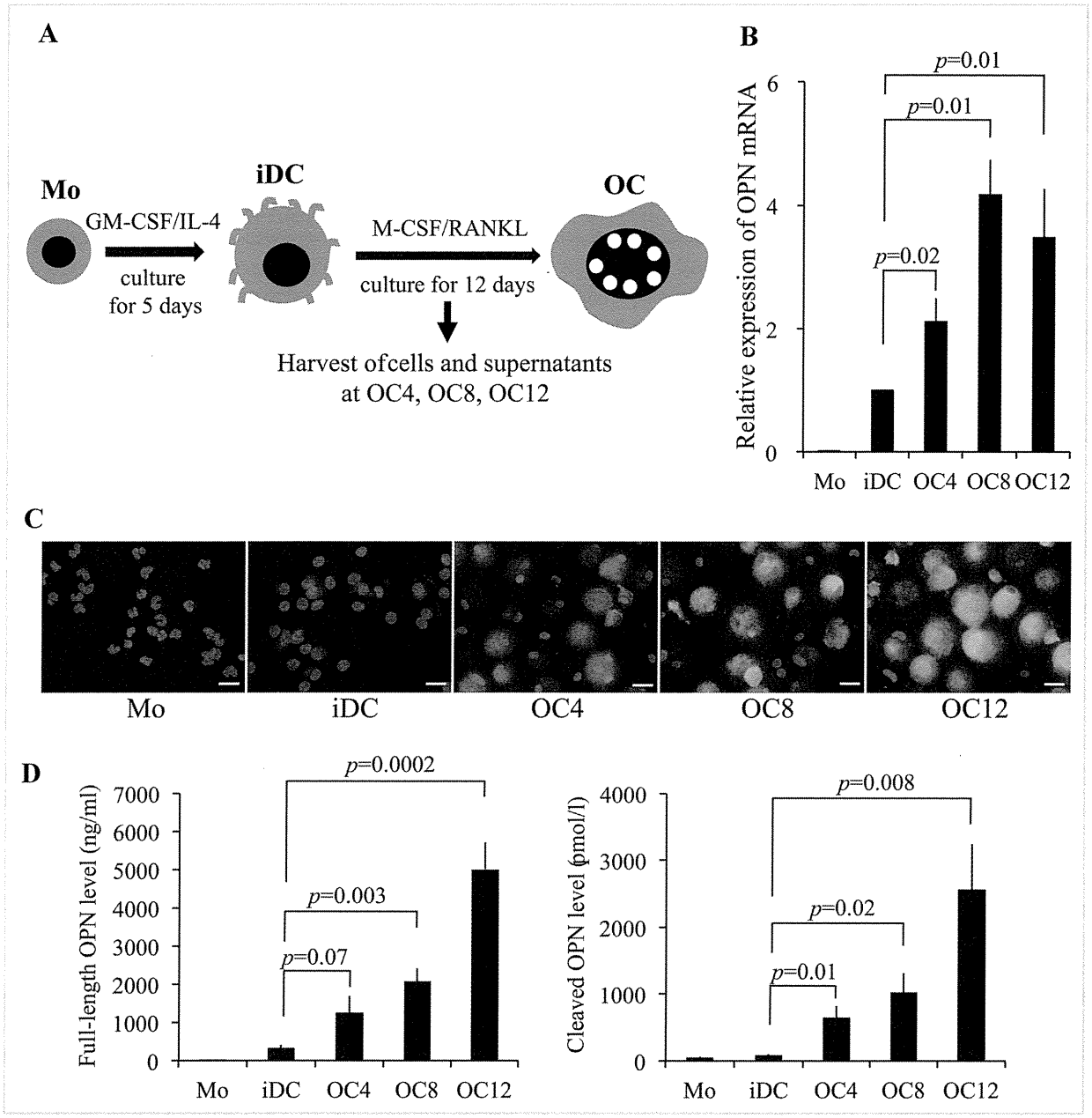

Fig. 1. OPN production in the course of OC-like MGC formation from iDCs in vitro. A: Schema of experimental design. Monocytes were purified from the peripheral blood of healthy adult volunteer donors. Monocyte-derived immature dendritic cells were generated in vitro by culturing for 5 days with GM-CSF/IL-4. Osteoclasts were generated in vitro by culturing iDCs for 12 days with M-CSF/RANKL. Cells and supernatants were harvested from the starting population of monocytes, the resultant iDCs, and OC-like MGCs on day 4, day 8, and day 12 of culture. B: OPN mRNA expression measured by relative quantitative RT-PCR (data shown are the mean of experiments with cells from five donors). Error bars represent mean ± SEM. C: Immunofluorescence staining with anti-OPN antibody (green) and DAPI (blue) performed on Mo, iDC, OC4, OC8, and OC12. Bars: 20 μm. D: Full-length and cleaved OPN in the cell culture supernatants of OC differentiation from iDCs (independent experiments with cells from eight donors). Error bars represent mean of the eight experiments ± SEM. GM-CSF, granulocyte-macrophage colony-stimulating factor; iDC, immature dendritic cell; M-CSF, macrophage colony-stimulating factor; MGC, multinucleated giant cell; Mo, monocyte; OC: osteoclast; OC4, OC-like MGCs on day 4; OC8, OC-like MGCs on day 8; OC12, OC-like MGCs on day 12; OPN, osteopontin; RANKL, receptor activator of NF-κB ligand; siRNA, small interfering RNA.

OPN mRNA, but the level expressed by iDCs was exceeded by differentiation stage OC8 (Fig. 1B). To characterize the OPN-producing cells further, we performed immunofluorescence staining on samples of each cell population (monocytes, iDCs, OC4, OC8, and OC12). Monocytes and iDC were attached to slide glass by cytospin. OC4, OC8, and OC12 were cultured on glass coverslips. In accordance with the increase in OPN mRNA expression found over the course of culture, production of OPN increased with differentiation: monocytes did not produce OPN, iDCs started to produce relatively small amounts, and OC12 produced the highest levels of OPN (Fig. 1C). The concentration of both the full-length and the cleaved forms of OPN in the cell supernatant steadily increased during the course of OC-like MGC formation (Fig. 1D).

EXPRESSION OF OPN RECEPTORS DURING THE COURSE OF OC-LIKE MGC GENERATION FROM iDCs

Next, we investigated the expression of receptors for OPN, specifically αvβ3 integrin, CD44v6, and α9β1 integrin, during the course of OC-like MGC formation. The mRNA levels of αvβ3 integrin, CD44v6, and α9β1 integrin increased and peaked at OC8 or OC12 (Fig. 2A), following a similar pattern to OPN production. CD44v6 mRNA was highly expressed by monocytes; however, its expression by iDCs was low. To characterize OPN receptor-expressing cells further we examined αvβ3-, CD44v6-, and α9β1-expressing OC12 for TRAP and OPN expression using immunofluorescence staining. Furthermore, to know whether iDCs remain at the end of culture, OC12, and whether the remaining iDCs are involved in the formation of OC-like

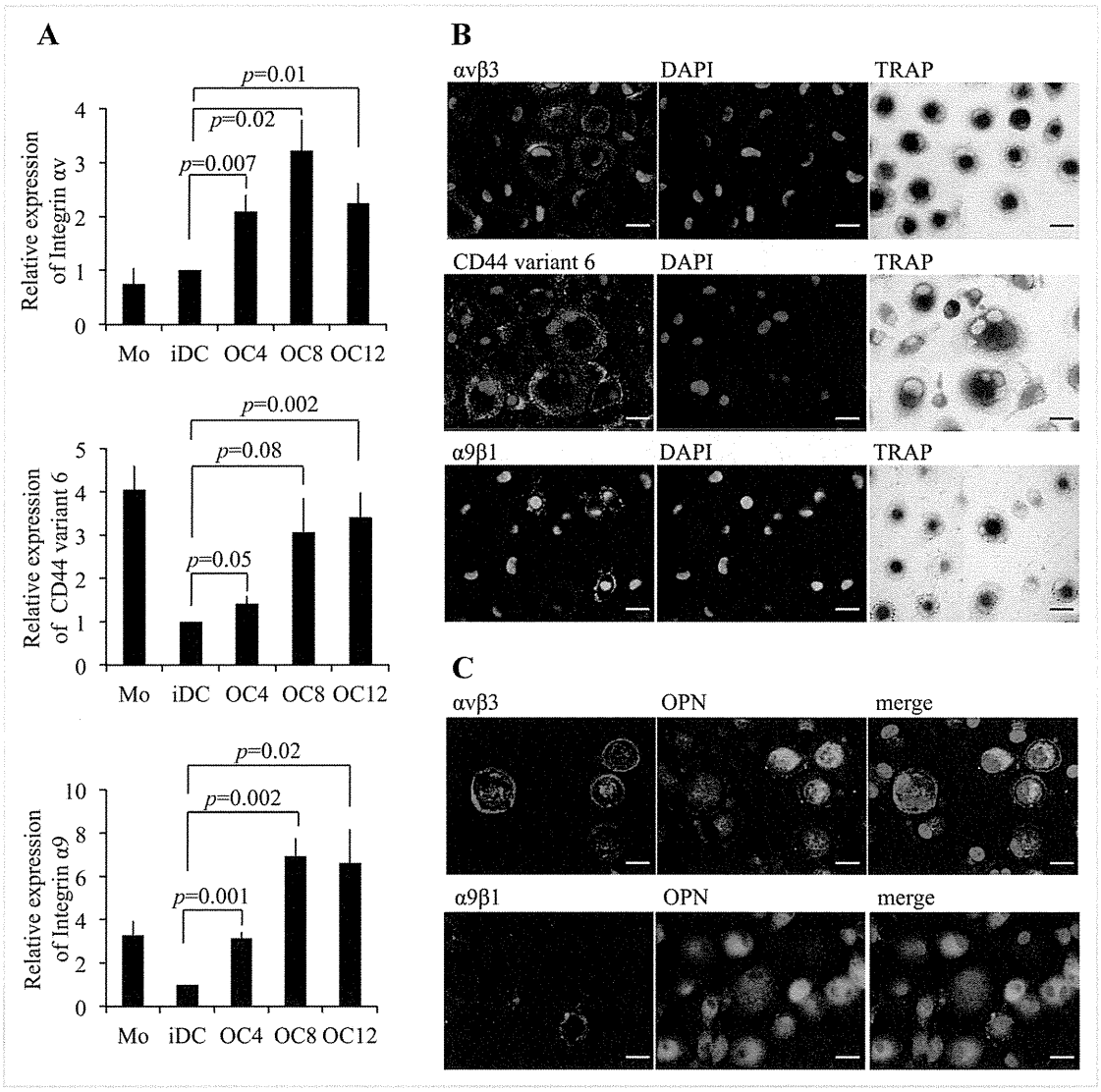

Fig. 2. OPN receptor expression during the course of OC-like MGC formation from iDCs and characterization of αvβ3-, CD44v6-, and α9β1-expressing cells. A: Expression of integrin αv mRNA (receptor for full-length OPN), CD44v6 mRNA (receptor for full-length OPN), and integrin α9 mRNA (receptor for cleaved OPN) measured by relative quantitative RT-PCR (data shown are the mean of experiments with cells from five donors). Error bars represent mean ± SEM. B: Detection of αvβ3, CD44v6 (receptors for full-length OPN), and α9β1 (receptor for cleaved OPN) by immunofluorescence staining (green) of OC12. Nuclei were stained with DAPI (blue). TRAP activity was assessed on the same glass coverslips. Bars: 20 μm. Data shown are representative of ten experiments. C: Detection of OPN (green) and its receptor (red) by double immunofluorescence staining. Nuclei were stained with DAPI (blue). Bars: 20 μm. Data shown are representative of 10 experiments. DAPI, 4′,6-diamidino-2-phenylindole; TRAP, tartrate-resistant acid phosphatase.

MGCs, we stained iDC marker, CD1a. Cells expressing αvβ3 were both TRAP- and OPN-positive but CD1a-negative, and some were multinucleated but with no more than four nuclei (Figs. 2B,C and 3A), suggesting that they were not fully mature OC-like MGCs. CD44v6-expressing cells were also TRAP-positive, and most were typical MGCs (Fig. 2B), suggesting that they were mature OC-like MGCs. On the other hand, α9β1-expressing cells were both OPN- and CD1a-positive but TRAP-negative with a single nucleus, and some were spindle shaped with processes characteristic of iDCs (Figs. 2B,C and 3A). Using fluorescence intensity scoring, we showed that cells expressing α9β1 existed before the start of OC differentiation and some iDCs expressed α9β1 integrin weakly but, while its expression became stronger during the course of OC-like MGC formation (Fig. 3B, Supplementary Fig. S1). The number of α9β1- and CD1a-positive cells did not increase (Fig. 3C,D). These data indicate that some remaining iDCs express α9β1 integrin strongly instead of the increased number of α9β1-positive cells. This suggests that α9β1- and CD1a-positive cells might have some role in OC-like MGCs formation.

OC-LIKE MGC FORMATION IS SUPPRESSED BY DOWN-REGULATION OF OPN

To study the role of OPN in OC-like MGC formation, we down-regulated the expression of OPN by transfection with OPN siRNA at the initial monocyte stage, or at the iDC stage (Fig. 4A). First, we generated iDCs from monocytes that had been transfected with either OPN siRNA or control siRNA. There was no difference in efficacy of differentiation of monocytes into iDCs between monocytes transfected with OPN siRNA or control siRNA, as judged by the expression of CD1a (Supplementary Fig. S2). Next, we prepared two types of iDCs, one derived from monocytes that had been treated with OPN

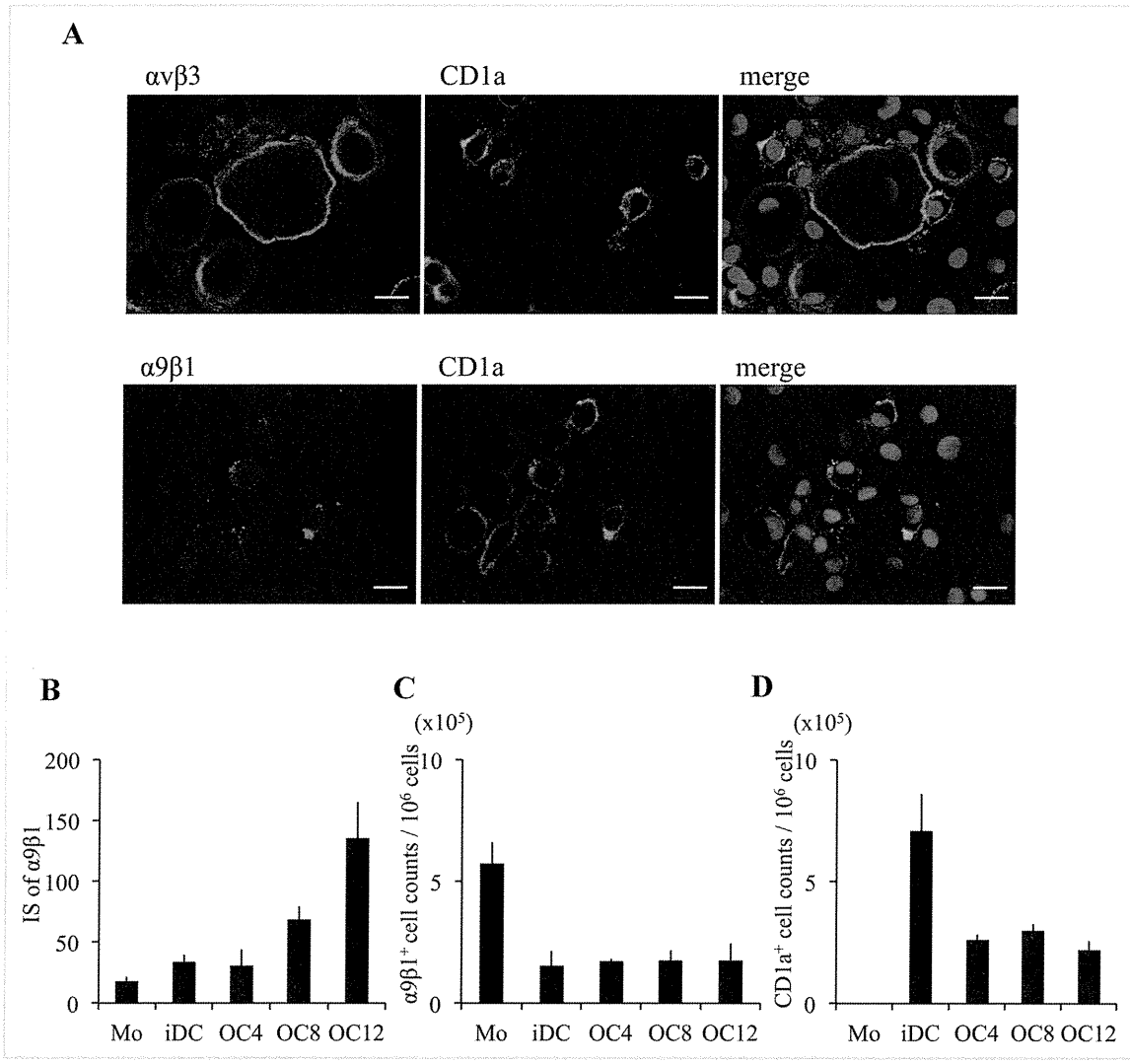

Fig. 3. The relationship between OPN receptors and CD1a. A: Detection of CD1a (green) and OPN receptors (red) by double immunofluorescence staining, Nuclei were stained with DAPI (blue). Bars: 20 μm. Data shown are representative of 10 experiments. B: Immunofluorescence data providing the IS of α9β1 expressed. The mean staining intensity was calculated as follows: IS, mean of brightness of selected cells' red channel score (in arbitrary units, AU) using Adobe Photoshop Elements, version 11. Data shown are the mean of experiments with cells from three donors. Error bars represent mean ± SEM. C: Number of α9β1-positive cells per 1×10^6 cells (data shown are the mean of experiments with cells from three donors). D: Number of CD1a-positive cells per 1×10^6 cells (data shown are the mean of experiments with cells from three donors). IS, intensity score.

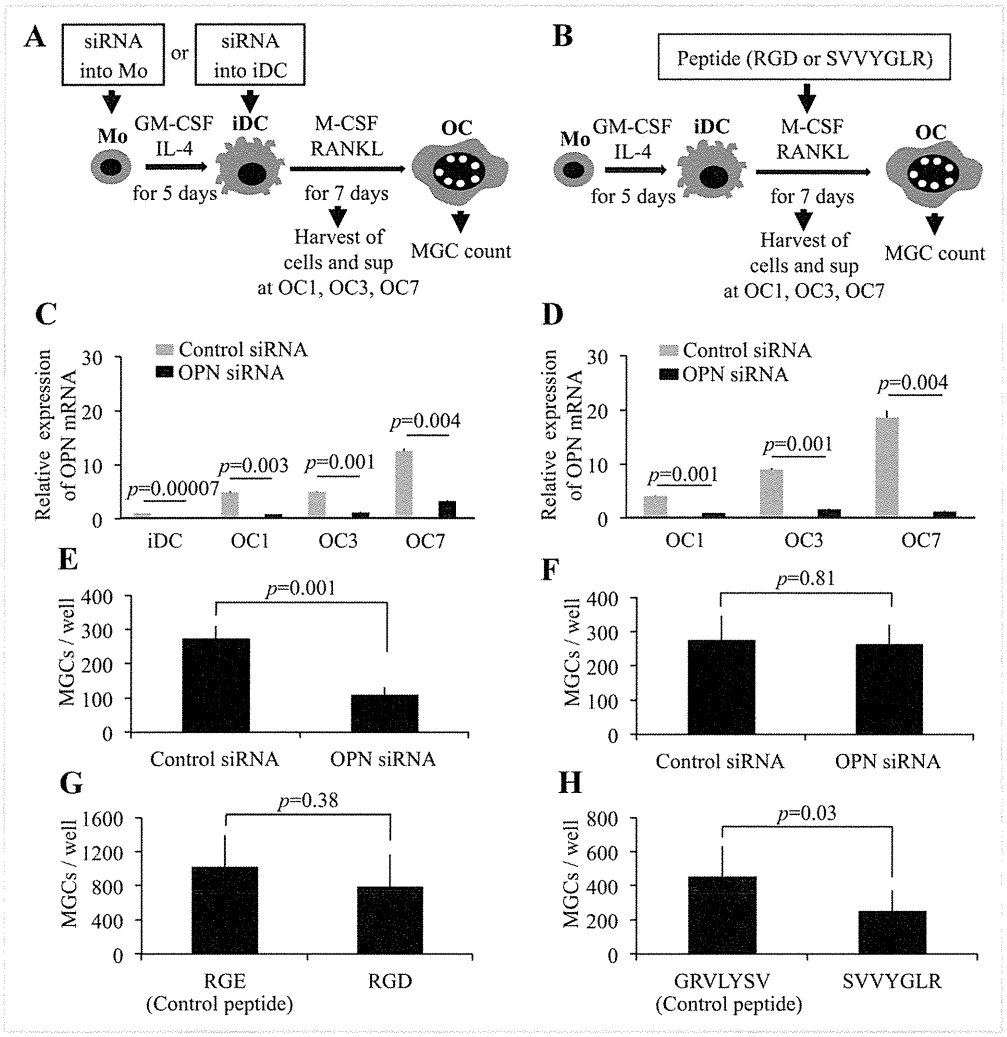

Fig. 4. The effect on MGC formation from iDC of down-regulating OPN with siRNA and inhibiting OPN binding. A: To study the role of OPN on OC-like MGC generation, OPN expression was down-regulated by transfection of OPN siRNA into monocytes or iDCs derived from non-treated monocytes. B: To identify the type of OPN receptor involved in MGC generation, two different synthetic peptides, RGD or SVVYGLR, were included in the culture medium during the differentiation of iDCs into OC-like MGCs. C, D: OPN mRNA levels measured by relative quantitative RT-PCR in OC-like MGC generated from (C) siRNA-transfected monocytes (data shown are the mean of experiments with cells from ten donors) or (D) siRNA-transfected iDCs (data shown are the mean of experiments with cells from ten donors). E, F: Number of MGCs differentiated from (E) iDCs generated from siRNA-transfected monocytes (data shown are the mean of experiments with cells from ten donors) or (F) siRNA-transfected iDCs (data shown are the mean of experiments with cells from ten donors). The number of MGCs was counted at OC7. G: Number of MGCs differentiated from iDCs in the presence of 10 μg/ml RGE (control) or RGD peptides (data shown are the mean of experiments with cells from five donors). H: Number of MGCs differentiated from iDCs in the presence of 1 μg/ml GRVLYSV (control) or SVVYGLR peptides (data shown are the mean of experiments with cells from six donors). MGCs were counted at OC7. Error bars represent mean ± SEM. OC1, OC-like MGCs on day 1; OC3, OC-like MGCs on day 3; OC7, OC-like MGCs on day 7; sup, supernatants.

siRNA (Fig. 4C,E), and the other derived from non-treated monocytes, which were treated with OPN siRNA at the iDC stage (Fig. 4D,F). Subsequently both types of iDCs were cultured for a further 7 days. Cells and supernatants were recovered at day 1, 3, and 7 and thus these cells were referred to as OC1, OC3, and OC7, respectively. The numbers of OC-like MGCs were counted on day 7 (OC7). With the exception of OC1, the concentration of full-length and cleaved forms of OPN in the supernatant of cells differentiated from both types of iDCs was reduced in OPN siRNA-transfected cells compared to cells transfected with control siRNA (Supplementary Fig. S3). Nevertheless, OPN mRNA expression was efficiently reduced by OPN siRNA treatment (Fig. 4C,D). By the end of culture on day 7, there was a significant reduction in MGC formation by iDCs derived from monocytes treated with OPN siRNA (Fig. 4E), while OPN siRNA-treated iDCs derived from non-treated monocytes were able to generate MGCs (Fig. 4F). These data suggest that OPN plays a role in the early phase of OC and/or MGC differentiation, specifically during the differentiation of monocytes to iDCs.

MGC FORMATION IS REDUCED BY SVVYGLR PEPTIDES

To investigate the type of OPN receptor involved in MGC formation, we used two different synthetic peptides, corresponding to internal

sequences of OPN, namely RGD, which binds RGD-recognizing integrins including αvβ3 and α5β1, and SVVYGLR, which is recognized by α4β1 and α9β1. These peptides were added to the culture medium during the differentiation of iDCs into OC-like MGCs (Fig. 4B). No obvious effect on MGC formation by RGD peptide compared to the RGE control peptide was observed (Fig. 4G). However, MGC formation was significantly reduced by SVVYGLR peptide as compared to the GRVLYSV control peptide (Fig. 4H), suggesting that α4β1 and/or α9β1 integrin receptors play a pivotal role in MGC formation.

OPN DID NOT AFFECT VIABILITY AND APOPTOSIS IN OC-LIKE MGC FORMATION

OPN is known to confer resistance to apoptosis [Tuck et al., 2007; Yamaguchi et al., 2013]. In inflammatory bone diseases, osteolytic lesions can be treated with bisphosphonates [Morimoto et al., 2011], which induce OC apoptosis [Abe et al., 2012]. Based on these reports, we hypothesized that OPN promote the survival and inhibit the apoptosis of OC precursor cells or OCs, consequently OC-like MGC formation is increased. We evaluated whether OPN affects cell viability and apoptosis in the course of OC-like MGC formation, using OPN siRNA-transfected or control siRNA-transfected monocyte-derived iDC. We determined cell viability and apoptosis by flow cytometry for floating cell and trypan blue stain and TUNEL stain for tightly adhering cells. Additionally, we performed Caspase-3 activity assay. Caspase-3 is an active cell-death protease involved in the execution phase of apoptosis, where cells undergo morphological changes such as DNA fragmentation, chromatin condensation, and apoptotic body formation [Porter and Janicke, 1999]. The number of viable cell and apoptotic cell, and caspase-3 activity were not affected by down-regulation of OPN (Fig. 5A–C).

OXIDATIVE STRESS IS NOT INVOLVED IN OPN PRODUCTION DURING THE COURSE OF OC-LIKE MGC FORMATION

In view of previous reports demonstrating that reactive oxygen species (ROS) may play a significant role as second messengers for the expression of osteopontin in mice [Umekawa et al., 2009; Lyle et al., 2012], it is an interesting issue whether ROS is linked to OPN production in human primary cells. To answer this question, we examined intracellular ROS activity and OPN production with or without ROS inhibitor of diphenyleneiodonium chloride (DPI) or *N*-acetyl-L-cysteine (NAC) in our culture system. DPI is a competitive inhibitor of flavin-containing cofactors and a very potent inhibitor of NADPH oxidase [Hancock and Jones, 1987]. NAC, in contrast, acts as a scavenger of ROS regardless of the source of production [Aruoma et al., 1989]. ROS was already generated at the differentiation into iDCs from monocytes, and came up to the highest levels at OC7 (Fig. 6A). As previous research has indicated [Del Prete et al., 2008], iDC differentiation from monocyte was suppressed when monocytes were pretreated with ROS inhibitor (Supplementary Fig. S4). We next treated iDCs with a non-cytotoxic concentration of DPI (100 nM) or NAC (20 mM), and evaluated the effect of ROS inhibitors on OPN production. Although ROS activity was significantly suppressed at OC7 (Fig. 6B), OPN production was not decreased (Fig. 6C,D). Because OPN is also known to reduce intracellular ROS during hypoxia/reperfusion to protect cells from oxidative injury [Denhardt et al., 1995], we examined intracellular ROS activity with or without down-regulation of OPN during the course of OC-like MGC formation. The down-regulation of OPN did not affect intracellular ROS activity (Supplementary Fig. S5).

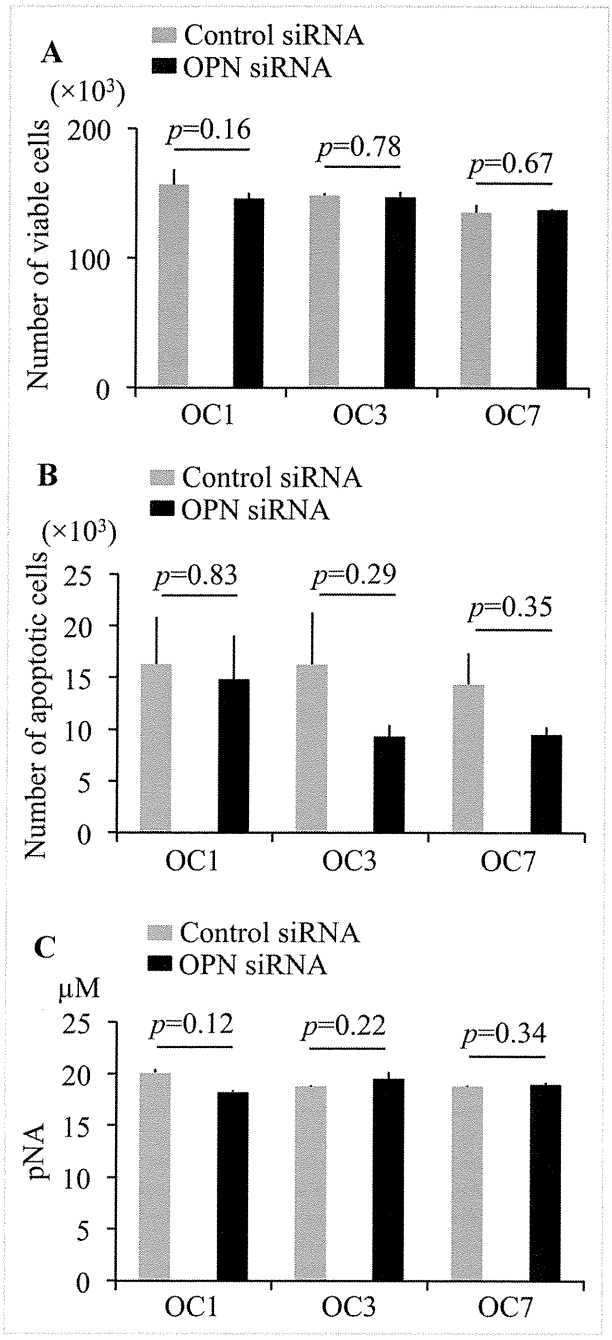

Fig. 5. Viability and apoptosis in the course of OC-like MGC differentiation from iDC of down-regulating OPN with siRNA. A: Number of viable cells. B: Number of apoptotic cells. C: Quantification of caspase-3 activity. We detected pNA as cleavage product by caspase-3. Data shown are the mean of experiments with cells from four donors. Error bars represent mean ± SEM. pNA, p-nitroaniline.

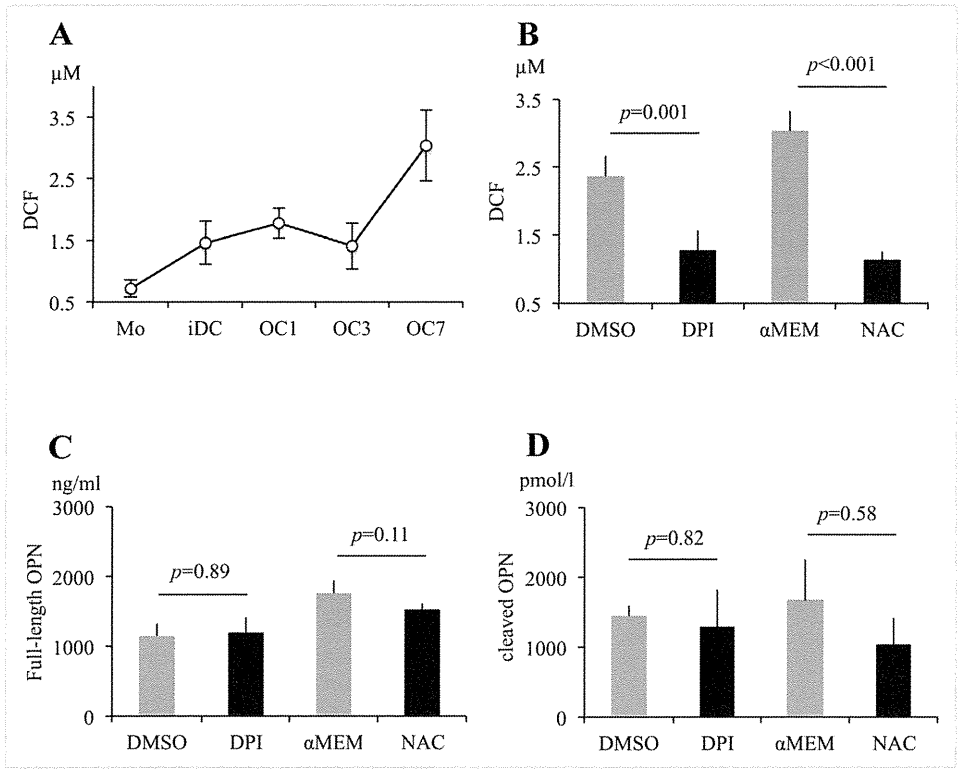

Fig. 6. The relation between ROS activity and OPN production. A: ROS activity during the course of MGC formation. We detected DCF as oxidized product by intracellular ROS. B: The effect of ROS inhibitor at OC7. C: Full-length OPN in the supernatants at OC7 differentiated from DPI- or NAC-treated iDC. D: Cleaved OPN in the supernatants at OC7 differentiated from DPI- or NAC-treated iDC. Data shown are the mean of experiments with cells from four donors. Error bars represent mean ± SEM. DCF, 2′, 7′-dichlorodihydrofluorescein; α-MEM, α-minimum essential medium; DMSO, Dimethyl sulfoxide; DPI, diphenyleneiodonium chloride; NAC, N-acetyl-L-cysteine.

DISCUSSION

In this study, we found that during the course of OC-like MGC formation from iDC, a large amount of OPN (both mRNA and protein) was produced, the cultured cells expressed OPN receptors, and inhibiting OPN expression suppressed OC-like MGC formation. These results indicate that OPN plays an important role in OC-like MGC formation from iDCs.

All cells expressed OPN during the course of OC-like MGC formation from iDCs in vitro. On the other hand, OPN receptors that recognize full-length OPN were expressed on TRAP-positive and CD1a-negative multinucleated cells, while the α9β1 integrin receptor, which recognizes the cleaved form of OPN, was expressed on TRAP-negative and CD1a-positive mononuclear cells. This indicates that full-length OPN stimulates cells that have differentiated into OC-like MGCs, while the cleaved form of OPN stimulates cells that have retained the character of iDCs. MGC formation from iDCs transfected with OPN siRNA was not suppressed, but that from iDCs generated from OPN-transfected monocytes was significantly suppressed. The differentiation of monocytes into iDCs was not itself influenced by OPN suppression. This indicates that OPN is crucial for OC-like MGC formation during the early phase, although OPN levels in OC1 cell culture supernatants were not significantly different between OPN siRNA- and control siRNA-transfected cells. There is a possibility that a critical OPN level for iDC fusion and OC-like MGC formation exists in the early phase of culture. MGC formation was not suppressed by the RGD peptide, which interferes with the interaction of full-length OPN with its receptor, but was significantly suppressed by SVVYGLR peptide, which interferes with the interaction of the cleaved form of OPN with its receptor. These findings suggest that cleaved OPN has a key role in stimulating iDC to differentiate into OC-like MGCs in an autocrine manner.

OPN has been known as a multi-functional secreted phosphoglycoprotein, which is involved not only in bone resorption by OCs but also in the immune defense system and autoimmune disease. Recently, an increasing number of reports describe the association between OPN and the inflammatory bone disease of RA and LCH. In mouse models of collagen-induced arthritis, OPN deficiency prevents development of the disease [Yumoto et al., 2002] and anti-OPN antibody, which blocks the interaction of OPN with its integrins, significantly inhibits disease development [Yamamoto et al., 2007]. Bronchoalveolar lavage cells from patients with pulmonary LCH spontaneously produce abundant amounts of OPN and OPN overexpression in rat lungs induces lesions similar to pulmonary LCH, with marked alveolar and interstitial accumulation of Langerhans cells [Prasse et al., 2009]. Furthermore, OPN is highly overexpressed in T cells and LCH cells of the LCH lesion [Allen et al., 2010].

T cells and antigen-presenting cells, such as DCs and macrophages, secrete OPN causing autocrine or paracrine stimulation that results in the secretion of other pro-inflammatory cytokines. This pro-

inflammatory action is more strongly induced by cleaved than full-length OPN [Uede, 2011]. For example, it was reported that the production by vascular smooth-muscle cells of free radicals related to oxidative stress was greater in response to cleaved OPN than in response to full-length OPN [Lai et al., 2006]. The adhesive ability of the cleaved OPN is also enhanced in comparison to that of full-length OPN [Gao et al., 2004]. Cleaved OPN and its receptors (the $\alpha4\beta1$ and $\alpha9\beta1$ integrins) are involved in the neutrophil infiltration and hepatic injury in inflammatory liver diseases [Diao et al., 2004]. Additionally, the cleaved form of OPN plays a critical role in RA [Morimoto et al., 2010; Uede, 2011], while a role for the cleaved form of OPN in LCH has not been revealed. In this paper, we demonstrate the role of cleaved OPN in the formation of OC-like MGCs from iDCs. Cleaved OPN could therefore plausibly play a role in the pathogenesis of both RA and LCH in which OCs are intimately involved [Redlich et al., 2002; da Costa et al., 2005].

OPN did not affect viability and apoptosis in OC-like MGC formation, suggesting OPN directly acts as a signal mediator for OC-like MGC formation. ROS activity increased during OC-like MGC formation, however, we could not discover any relation between ROS activity and OPN production.

ACKNOWLEDGMENTS

This study was supported by a grant for Research on Measures for Intractable Diseases from the Ministry of Health, Labor and Welfare, Japan and Grant-in-Aid for Scientific Research (KAKENHI) from the Ministry of Education, Culture, Sports, Science and Technology, Japan. This study was carried out under the Joint Research Program of the Institute for Genetic Medicine, Hokkaido University, and with funds from the JKA Foundation raised through its promotion of KEIRIN RACE. We thank Dr. Hiroko Hayakawa, of JMU Core Center of Research Apparatus, for help with flow cytometry.

REFERENCES

Abe K, Yoshimura Y, Deyama Y, Kikuiri T, Hasegawa T, Tei K, Shinoda H, Suzuki K, Kitagawa Y. 2012. Effects of bisphosphonates on osteoclastogenesis in RAW264.7 cells. Int J Mol Med 29:1007–1015.

Allen CE, Li L, Peters TL, Leung HC, Yu A, Man TK, Gurusiddappa S, Phillips MT, Hicks MJ, Gaikwad A, Merad M, McClain KL. 2010. Cell-specific gene expression in Langerhans cell histiocytosis lesions reveals a distinct profile compared with epidermal Langerhans cells. J Immunol 184:4557–4567.

Aruoma OI, Halliwell B, Hoey BM, Butler J. 1989. The antioxidant action of N-acetylcysteine: Its reaction with hydrogen peroxide, hydroxyl radical, superoxide, and hypochlorous acid. Free Radic Biol Med 6:593–597.

Chapuis F, Rosenzwajg M, Yagello M, Ekman M, Biberfeld P, Gluckman JC. 1997. Differentiation of human dendritic cells from monocytes in vitro. Eur J Immunol 27:431–441.

Chellaiah MA, Kizer N, Biswas R, Alvarez U, Strauss-Schoenberger J, Rifas L, Rittling SR, Denhardt DT, Hruska KA. 2003. Osteopontin deficiency produces osteoclast dysfunction due to reduced CD44 surface expression. Mol Biol Cell 14:173–189.

da Costa CE, Annels NE, Faaij CM, Forsyth RG, Hogendoorn PC, Egeler RM. 2005. Presence of osteoclast-like multinucleated giant cells in the bone and nonostotic lesions of Langerhans cell histiocytosis. J Exp Med 201:687–693.

Del Prete A, Zaccagnino P, Di Paola M, Saltarella M, Oliveros Celis C, Nico B, Santoro G, Lorusso M. 2008. Role of mitochondria and reactive oxygen species in dendritic cell differentiation and functions. Free Radic Biol Med 1:1443–1451.

Denhardt DT, Lopez CA, Rollo EE, Hwang SM, An XR, Walther SE. 1995. Osteopontin-induced modifications of cellular functions. Ann NY Acad Sci 760:127–142.

Diao H, Kon S, Iwabuchi K, Kimura C, Morimoto J, Ito D, Segawa T, Maeda M, Hamuro J, Nakayama T, Taniguchi M, Yagita H, Van Kaer L, Onóe K, Denhardt D, Rittling S, Uede T. 2004. Osteopontin as a mediator of NKT cell function in T cell-mediated liver diseases. Immunity 21:539–550.

Gao C, Guo H, Downey L, Marroquin C, Wei J, Kuo PC. 2003. Osteopontin-dependent CD44v6 expression and cell adhesion in HepG2 cells. Carcinogenesis 24:1871–1878.

Gao YA, Agnihotri R, Vary CP, Liaw L. 2004. Expression and characterization of recombinant osteopontin peptides representing matrix metalloproteinase proteolytic fragments. Matrix Biol 23:457–466.

Green PM, Ludbrook SB, Miller DD, Horgan CM, Barry ST. 2001. Structural elements of the osteopontin SVVYGLR motif important for the interaction with alpha(4) integrins. FEBS Lett 503:75–79.

Hancock JT, Jones OT. 1987. The inhibition by diphenyleneiodonium and its analogues of superoxide generation by macrophages. Biochem J 242:103–107.

Hu DD, Lin EC, Kovach NL, Hoyer JR, Smith JW. 1995. A biochemical characterization of the binding of osteopontin to integrins alpha v beta 1 and alpha v beta 5. J Biol Chem 270:26232–26238.

Lai CF, Seshadri V, Huang K, Shao JS, Cai J, Vattikuti R, Schumacher A, Loewy AP, Denhardt DT, Rittling SR, Towler DA. 2006. An osteopontin-NADPH oxidase signaling cascade promotes pro-matrix metalloproteinase 9 activation in aortic mesenchymal cells. Circ Res 98:1479–1489.

Lyle AN, Joseph G, Fan AE, Weiss D, Landázuri N, Taylor WR. 2012. Reactive oxygen species regulate osteopontin expression in a murine model of postischemic neovascularization. Arterioscler Thromb Vasc Biol 32:1383–1391.

Morimoto A, Shioda Y, Imamura T, Kanegane H, Sato T, Kudo K, Nakagawa S, Nakadate H, Tauchi H, Hama A, Yasui M, Nagatoshi Y, Kinoshita A, Miyaji R, Anan T, Yabe M, Kamizono J. 2011. Nationwide survey of bisphosphonate therapy for children with reactivated Langerhans cell histiocytosis in Japan. Pediatr Blood Cancer 56:110–115.

Morimoto J, Kon S, Matsui Y, Uede T. 2010. Osteopontin; as a target molecule for the treatment of inflammatory diseases. Curr Drug Targets 11:494–505.

Murakami I, Morimoto A, Oka T, Kuwamoto S, Kato M, Horie Y, Hayashi K, Gogusev J, Jaubert F, Imashuku S, Al-Kadar LA, Takata K, Yoshino T. 2013. IL-17A receptor expression differs between subclasses of Langerhans cell histiocytosis, which might settle the IL-17A controversy. Virchows Arch 462:219–228.

Porter AG, Janicke RU. 1999. Emerging roles of caspase-3 in apoptosis. Cell Death Differ 6:99–104.

Prasse A, Stahl M, Schulz G, Kayser G, Wang L, Ask K, Yalcintepe J, Kirschbaum A, Bargagli E, Zissel G, Kolb M, Müller-Quernheim J, Weiss JM, Renkl AC. 2009. Essential role of osteopontin in smoking-related interstitial lung diseases. Am J Pathol 174:1683–1691.

Redlich K, Hayer S, Ricci R, David JP, Tohidast-Akrad M, Kollias G, Steiner G, Smolen JS, Wagner EF, Schett G. 2002. Osteoclasts are essential for TNF-alpha-mediated joint destruction. J Clin Invest 110:1419–1427.

Rivollier A, Mazzorana M, Tebib J, Piperno M, Aitsiselmi T, Rabourdin-Combe C, Jurdic P, Servet-Delprat C. 2004. Immature dendritic cell transdifferentiation into osteoclasts: A novel pathway sustained by the rheumatoid arthritis microenvironment. Blood 104:4029–4037.

Smith LL, Cheung HK, Ling LE, Chen J, Sheppard D, Pytela R, Giachelli CM. 1996. Osteopontin N-terminal domain contains a cryptic adhesive sequence recognized by alpha9beta1 integrin. J Biol Chem 271:28485–28491.

Standal T, Borset M, Sundan A. 2004. Role of osteopontin in adhesion, migration, cell survival and bone remodeling. Exp Oncol 26:179–184.